Masters Program in Geospatial Technologies

Deep Learning for Studying Urban Water Bodies' Spatio-temporal Transformation: A Study of Chittagong City, Bangladesh

Muhammad Esmat Enan

Dissertation submitted in partial fulfilment of the requirements for the Degree of *Master of Science in Geospatial Technologies*

NOVA IMS
UNIVERSITAT JAUME·I
WESTFÄLISCHE WILHELMS-UNIVERSITÄT MÜNSTER

Deep Learning for Studying Urban Water Bodies' Spatio-temporal Transformation: A Study of Chittagong City, Bangladesh

Supervised by

Filiberto Pla Bañón, PhD
Professor, Institute of New Imaging Technologies (INIT)
Universitat Jaume I (UJI)
Castellon de la Plana, Spain

Co-supervised by

Rubén Fernández Beltrán, PhD
Institute of New Imaging Technologies (INIT)
Universitat Jaume I (UJI)
Castellon de la Plana, Spain

Co-supervised by

Mário Silvio Rochinha de Andrade Caetano, PhD
Associate Professor, Nova Information Management School
Universidade Nova de Lisboa (UNL)
Lisbon, Portugal

Date of Submission

February 21, 2021

DEDICATED TO
MY PARTENTS

ACKNOWLEDGEMENT

In the successful completion of this thesis, I thank the creator **Allah Subhanahu Wa Ta'ala** (Alhamdulillah). Then, I like to express my heartiest reverence to my honorable thesis supervisor **Prof. Dr. Filiberto Pla Bañón** for his scholastic guidance, encouragement, and providing suitable space to conduct the study in this pandemic situation.

Similarly, I am thankful to my co-supervisor, **Dr. Rubén Fernández Beltrán** for his continuous supervision, mental assistance, and constructive criticism throughout the study period. My heartiest gratitude goes to my co-supervisor, **Prof. Dr. Mário Silvio Rochinha de Andrade Caetano** for his valuable feedbacks and suggestions on thesis progress. I am feeling lucky for having all of them on my supervisory board.

I am also grateful to **Shimul Sarker**, **Shakhawat Hossain Shoel,** and **Obidur Rahman** for helping me to have the required auxiliary data for this study. I am specially thankful to the **Erasmus Mundus Program** for financing my entire journey of this MSc program. Besides, I grateful to **GeoTech Family** for giving me some wonderful memories to cherish for a lifetime.

Finally, I would like to extend my heartfelt thanks to all the members of my family, including my **parents**, **wife**, and all the hard-working **brothers** and **sisters,** whose dedication gave me moral support and made it possible to carry out the research.

Muhammad Esmat Enan
February, 2021

ABSTRACT

Water has been playing a key role in human life since the dawn of civilization. It is an integral part of our lives. In recent years, water bodies specially, urban water bodies are in a poor state due to climate change and rapid urban expansion. Though some cities have become aware of this poor state of water bodies, many cities around the world are not contemplating this issue. Because less research has been conducted on water bodies than other land covers in urban areas like built-up. Besides, many advanced algorithms are currently being utilized in different fields, but in terms of water body study, these advancements are still missing. That is why this study aims at investigating the spatio-temporal changes in urban water bodies in Chittagong city using deep learning and freely available Landsat data. Looking at the significance of the study, firstly, as this study has adopted two different deep learning (DL) models and evaluated the performance, the findings can help to understand the suitability of applying deep learning algorithms to extract information from mid to low resolution imagery like Landsat. Secondly, this work will help us to understand why the conservation of the existing water bodies is so important. Finally, this study will encourage further research in the field of deep learning and water bodies by opening the door for monitoring other environmental resources.

KEYWORDS

Artificial Neural Network
Convolution Neural Network
Deep Learning
Landsat data
Machine Learning
Urban Water bodies

ACRONYMS

AdaGrad	Adaptive Gradient
Adam	Adaptive Moment Estimation
ANN	Artificial Neural Network
ASTER	Advanced Spaceborne Thermal Emission and Reflection Radiometer
BMD	Bangladesh Meteorological Department
CCC	Chittagong City Corporation
CNN	Convolutional Neural Network
DEM	Digital Elevation Model
DL	Deep Learning
DN	Digital Number
DNN	Deep Neural Network
GDEM	Global Digital Elevation Model
GIS	Geographic Information system
GPAD	Geo-Planning for Advanced Development
GS	Global Scale
LS	Local Scale
MIR	Mid-infrared
ML	Machine Learning
MNDWI	Modified Normalized Difference Water Index
MOLUSCE	Modules for Land Use Change Simulations
MRI	Magnetic Resonance Imaging
MSS	Multispectral Scanner
NASA	National Aeronautics and Space Administration
NDWI	Normalized Difference Water Index
NIR	Near Infrared
NS	National Scale
OLI	Operational Land Imager
ReLU	Rectified Linear Unit
RMSProp	Root Mean Square Propagation
RS	Remote Sensing
SGD	Stochastic Gradient Descent
SWIR	Short-wave infrared

TIFF	Tag Image File Format
TIRS	Thermal Infrared Sensor
TM	Thematic Mapper
TOA	Top-of-Atmosphere.
USGS	United States Geological Survey

INDEX

INDEX OF FIGURES

INDEX OF TABLES

CHAPTER ONE
Introduction

1.1 Background of the Study

1.2 Research Gap and Motivation

1.3 Aim, Objectives and Research Questions

1.4 Significance of the Study

1.5 Chapter Overview

1.1 Background of the Study

Water is a basic requirement for sustaining the existence of all living organisms (Sharma et al., 2017). In urban areas, water bodies have higher evaporation rates than areas with green coverage (Mostafa and Manteghi, 2019). Therefore, water spaces play a key role to create cooling islands in urban areas, which results in the variation in temperature of the contiguous environment (Sun and Chen, 2012; Hathway and Sharples, 2012). Water bodies are always colder than the overlying air during the day time in warm weather (Gross, 2017; Broadbent et al., 2017) thus, urban water bodies can mitigate the temperature of the urban environment by reducing their energy taking tendency (Manteghi et al., 2016).

Most water bodies worldwide suffer from problems of contamination and invasion by manufacturing, urban and agricultural production. Urban population, agriculture, and industry are demanding increment of freshwater day by day. (Bogdanets and Vlaev, 2015). Likewise, the urban population also wants more land for housing, infrastructure growth and other purposes, which eventually stresses the water bodies. (Neelakantan and Ramakrishnan, 2017). It is said, urban growth is one of the main drivers of land cover transition, which has a significant effect on adjacent environment (Mostafa and Manteghi, 2019). Earth's surface transition to urban application showing the major shifts in global land use and land cover (Weng & Yang, 2004; Manteghi et al., 2015). We are altering water bodies by changing land use and land cover. The effects of this change depend on certain factors, such as the urban center's size, existing water bodies, city's historical and natural setting, etc. Although different scientific literature has shown the ecological effects of urban development on aquatic environments with approaches to restoration and problem mitigation (Hughes et al., 2014), we cannot see any practical utilization of these approaches. As a result, urban water bodies are being converted into other land covers, and water-related problems are becoming more prevalent in urban areas.

The accessibility of big data, advances in algorithms and rapid expansion in computing have led us to the powerful concept of ML in recent decades. ML algorithms are being used for various purposes, including the classification, regression, clustering, or reduction of complexity of big data, particularly high-dimensional input data processing (Schmidt et al., 2019). ML is a method of automatic learning that takes place by analyzing large datasets. By estimating mathematical functions, it learns to link one or more inputs to one or more outputs to predict a set of new data (Di Franco and Santurro, 2020; Jordan and Mitchell 2015); hence, this technique can be assessed to monitor water-related problems based satellite data.

1.2 Research Gap and Motivation

Throughout the world, the land cover type that has been mostly influenced by natural and human activates is water body. Encroachment, land use alteration, uncontrolled urbanization, and climate change are some of the factors that are trigging this influence. Most the these factors are driven by human i.e. most of the water bodies are being influenced by anthropogenic activities. Problems associated with urban water bodies are almost common throughout the world. Therefore, various conservation initiatives are being observed to protecting existing water bodies all over the world.

In Bangladesh, pollution is the major problem associated with urban water bodies because of which most of the water bodies become unusable. In most of the cities of this country, uncontrolled urbanization area converting water bodies into the built-up area/ constructed land. Different studies have reported that the second largest city of this country (Chittagong) is experiencing the same situation. In this city, water bodies are turning into constructed areas to provide housing for the city's growing population. In addition, factories located in and around the city are influencing urban water bodies both directly and indirectly.

Nowadays, to monitor the spatio-temporal changes in urban water bodies, modern technologies like; Geographical Information Systems (GIS), Remote sensing (RS) are very popular (Denning, 1993; Jeton &Smith,1993). Before that, studies like water resource modeling required some time-consuming steps (Tsihrintzis et al., 1996). Earth observatory satellite like Landsat provides opportunities to monitor changes in urban water bodies by offering mid to low resolution multi-spectral data Apart from modern technologies and remotely sensed data, advanced algorithms are also essential to monitor not only urban water bodies but also other environmental resources. CNN and DNN have recently shown the superiority of deep learning algorithms over conventional image classification algorithms as they can learn from multi-level representation. (Cai et al., 2018).

It is said, at present, studies on water body are less available than those of built-up, green landscape, and .other land covers (Yang et al., 2015). In addition, we can see the application of DL in different fields but, this technique is still to be utilized in urban water research specially, to check the spatio-temporal changes. So this study has been undertaken to fulfill this gap.

1.3 Aim, Objectives and Research Questions

The study aims to find out the spatio-temporal changes in urban water bodies in Chittagong city using DL. There are two specific objectives of the study which are given below:

1. To find out the changing trend in urban water bodies in the study area from 2000 to 2020.

2. To simulate the scenario (area coverage) of the urban water bodies in the study area for 2040.

In order to fulfill these objectives, the study has tried to search for the possible answers to the following questions.

- Based on past and present records, what is the general trend of changes in urban water bodies ?
  - This question shows the changing pattern of water bodies in the study area from 2000 to 2020.

- What will be the future scenario of the urban water bodies in that area?
  - This question discloses the upcoming condition of the water bodies in the city.

From the objectives and research questions it is clear that the main focus of this study is on changes in water bodies; but, in the result section, we are going to present the discussion on both water and non-water bodies. The reason is, without considering both water and non-water land cover, we cannot find out the changing scenario in the water bodies properly. If we remove non-water bodies from all the figures, it will create an empty space on the maps, logically which is not true. On the other hand, the presence of non-water parts in the figures without discussion will raise a question. In addition, our models (CNN and ANN) are also predicting two classless; a) water bodies and b) non-water bodies. So, we are going to discuss both water bodies and non-water bodies, given all these concerns. A summary of the notions of water bodies and non-water bodies in this study is shown in **Table 1.1.**

Table 1.1: Specification of water bodies and non-water bodies

Classification Types	**Specification**
Water bodies	River, wetland (permanent and seasonal), canal, stream, sea, low-land, marshy land, etc.
Non-water bodies	Others (e.g. residential area, commercial area, crop filed, bare land)

1.4 Significance of the Study

As it is mentioned in the research gap section, there have been limited studies on urban water bodies at both local and global scales; therefore, it is a timely and unavoidable research. At the **LS** (local scale), this work will highlight the changing scenario and the future status of urban water bodies in Chittagong. As a result, it will be easier to understand, why these water bodies need to be brought under conservation practice. At the **NS** (national scale), this work will be an example of how modern technology, such as deep learning, can be used to monitor environmental problems. Besides, methodology followed in this study will open the door to monitor other environmental issues. In addition, at the **GS** (global scale), this work will fill the absence of the application of deep learning in urban water body change monitoring. Finally, the study will also try to disclose whether DL is capable of monitoring environmental problems from low to mid resolution data like Landsat.

1.5 Chapter Overview

The thesis report is organized into six chapters. Each chapter contains in detail discussion about the different parts of the study.

Chapter **1** consists of a background, research gap, motivation, aim, objectives, research questions, and the significance of the research.

Chapter **2** represents the literature review and theoretical aspects, where; water bodies and their importance, popular techniques of studying spatio-temporal changes in water bodies, deep learning, artificial neural network, and selection of base architecture for the study are illustrated.

Chapter **3** is providing information about the study area and datasets used in this study.

Chapter **4** depicts the whole methodological workflow of the study in detail.

Chapter **5** includes the model performance, classification outputs, change analysis. Besides, this chapter also discloses the future condition of urban water bodies and their interaction with non-water bodies.

Finally, the closing chapter (chapter **6**) consists of the conclusion and future directions of the current study.

CHAPTER TWO

Literature Review and Theoretical Aspects

2.1 Introduction

2.2 Urban Water body and Its Importance

2.3 Popular Techniques of studying Spatio-temporal Changes

2.4 Deep Learning and CNN

2.5 Selection of Base Architecture

2.6 Training

2.7 Modified Architecture Adopted in this Study

2.8 Artificial Neural Network

2.9 ANN Architecture Adopted in the Study

2.1 Introduction

This chapter is showing the theoretical basement of this study. Definition of urban-water bodies, their roles, different components of CNN, ANN, and the adopted models of this study have been discussed here in detail. Besides, the functionalities of every single component are also placed here.

2.2 Urban Water body and Its Importance

In general, water body refers to the part of the earth's surface that is covered with water. So, urban water bodies can be defined as the part of the urban landscape covered with water. This landscape can be natural or artificial, permanent or temporary.

As an integral part of the ecology, one of the major functionalities of the urban water bodies is to support wildlife. Water bodies also contribute to the economy and scenic beauty of an urban area. In a riverine city, urban water bodies play vital roles to connect different parts of that city.

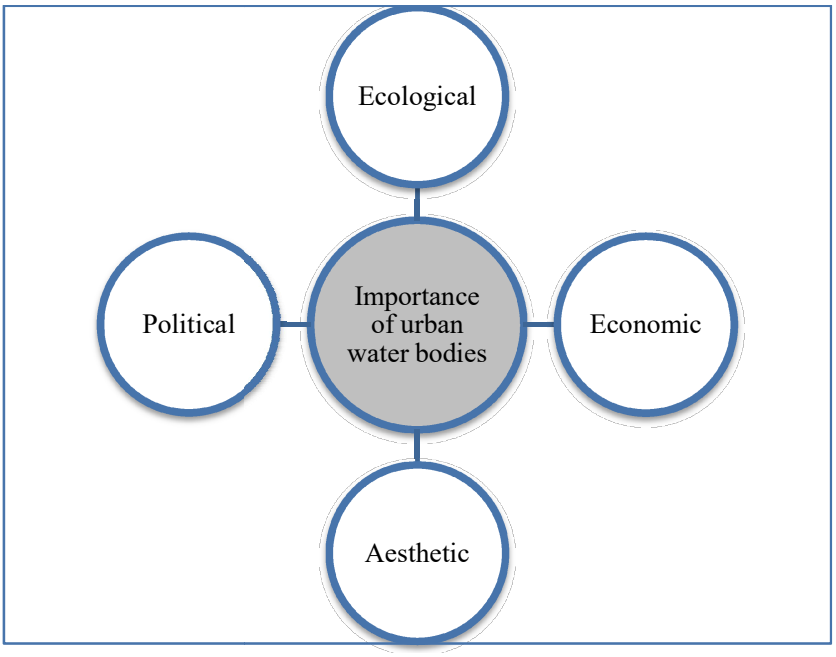

Figure 2.1: Significance of water bodies in urban areas

Geographically, some urban water bodies play a significant role to establish the political relationship between the two countries. In addition, Water bodies are intimately involved with a city because they play a key role in its growth and

maintenance. Water functions are not limited to domestic boundaries and waste discharge, as it also plays a vital role in ecology. (Milosevic and Winker, 2015).

2.3 Popular Techniques of Studying Spatio-temporal Changes

There are several techniques to explore the Spatio-temporal changes in water bodies from remotely sensed data. Two dominating techniques are image classification and index application.

Image classification can be either supervised or unsupervised. Unsupervised classification method does not require prior knowledge, while supervised classification needs real understanding of the land cover in the study area (Thompson and Mikhail, 1976; Ismail et al., 2009). Examples of supervised algorithms include: maximum likelihood classification, minimum distance classification, mahalanobis distance classification, etc (50 North, 2017). Similarly, K-means, ISODATA are commonly used unsupervised algorithms (GIS Geography, 2021).

The two most popular indices to identify the spatio-temporal changes in water bodies are NDWI and MNDWI.

The water features captured in NDWI involve false positives from constructed areas; therefore, a revised water index was developed. The new index can capture the water surface by minimizing errors from constructed land, forest, and soil (Ullah and Enan, 2016; Xu, 2006). Mathematically two indices can be shown as follow:

$$NDWI = (GREEN - NIR) / (GREEN + NIR) \quad 2.1$$

$$MNDWI = (GREEN - MIR) / (GREEN + MIR) \quad 2.2$$

Now, let's assume we want to calculate NDWI using Landsat 8 imagery. We need band 3 (GREEN) and band 5 (NIR); hence, the equation would be

$$NDWI = (B3 - B5) / (B3 + B5) \quad 2.3$$

Similarly, to calculate MNDWI from the same satellite imagery, we need band 3 (GREEN) and band 6 (MIR). This can be expressed as follow:

$$MNDWI = (B3 - B6) / (B3 + B6) \quad 2.4$$

2.4 Deep Learning and CNN

DL is a versatile ML subfield that solves a number of tasks, including image analysis, computer vision, signal processing, and speech recognition(LeCun et al., 2015). DL has the ability to automatically learn internal image representation from actual image at different levels, which is very helpful in classifying images and detecting objects. O'Mahony et al., (2019).

Over past years, a lot of scientific experiments have been applying DL for satellite imagery processing (Zhang., et al, 2015; Zhang., et al, 2016). DL proved to be capable of processing and extracting different land covers both form optical and radar images (Chen et al., 2014; Mnih and Hinton, 2010; Geng et al., 2015). One of the commonly used DL models is the Convolutional Neural Network (CNN) which has been widely utilized for different purposes including handwriting recognition from binary images (Ciresan et al., 2010), classification of hyperspectral, MRI, and multi-spectral data (Meszlény et al., 2017; Chen., et al 2014), learning from videos (Mobahi, 2009), crop classification (Ji et al., 2018) etc.

2.5 Selection of Base Architecture

The architecture (**Figure 2.2**) was selected as the guideline of the study, which was presented by Ji et al., (2018). Apart from input and output layer, this architecture contains convolution layer, pooling layer, and fully connected layer.

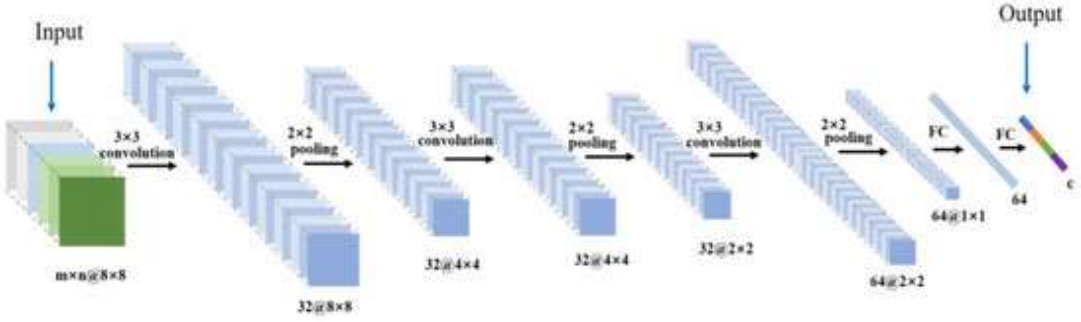

Figure 2.2: Selected 2D CNN architecture

Some commonly used components of CNN are discussed below.

2.5.1 The Convolution Layer: As CNN's main building block, convolution layers are applied to extract different features from imagery with the process learned by the network. More precisely, It is a method in which a small number or kernel matrix is passed over the image and interpreted depending on values from the image's filtered block. In this whole process the value is extracted based on following formula (Ganegedara, 2018).

$$h_{i,j} = \sum_{k=1}^{m} \sum_{l=1}^{m} w_{k,l} x_{i+k-1,j+l-1} \quad 2.5$$

Here,

m = width and height of window/kernel

h = output of convolution,

x = inputs

w= convolution kernel/window

To summarize, it can be said, a convolution layer applies the filters of specific dimension to perform convolution operations for scanning the input image.

2.5.2 Pooling Layer: This layer produces a new set of pooled feature maps from each feature map independently. It is a function that aims to minimize the quantity of the representations in order to progressively lessen the number of network parameters and computational complexity. This process includes the selection of a pooling operation similar to a filter adapted to feature map. The aspect of the feature map filter is bigger than the filter of the pooling operation (Pokharna, 2016;Geeksforgeeks, 2019).

Let's assume we have a feature map with height= y, width = x , and number of channels= c, now, after applying the pooling layer we will get an output with the following dimension:

$$\frac{(y - f + 1)}{s} \times \frac{(x - f + 1)}{s} \times c \quad 2.6$$

Where,
f = is size of filter and
s = is stride length

Two types of pooling operations exist: a) max-pooling and b) average-pooling. (Brownlee, 2019).

Table 2.1: Difference between max and average pooling

Categories	Max-pooling	Average-pooling
Purposes	Mmaximum value is selected by each pooling process when filtering	Each pooling operation averages the while filtering
Remarks	• Protects identified features • Very popular	• Reduces feature map • Mostly utilized in LeNet

Source: (Amidi, Amidi n.d.)

2.5.3 Dense or Fully Connected Layer: The dense or fully-connected layer is utilized to combine all the learned features of different convolution kernels to have a holistic image by building a global representation from the network (Singh, n.d.). So, in a neural network, the FC layer refers to a stage or a layer where each activation unit of next layer is linked to all inputs from previous layer. Generally, after adding multiple convolutions and pooling layers, the FC layer is installed at the end of the network..

2.5.4 Dropout Layer: This layer is associated with the technique of temporarily stopping the contribution of some randomly selected neurons to the activation function. So, the selected neurons are not considered for a particular pass (whether it is a forward pass or backward pass).

2.5.5 Flatten Layer: A flattening layer executes a function to convert the feature map to a one-dimensional array. More precisely, this process can flatten the output of the convolution layers into a single feature vector by putting all the pixel data in one line. The flatten output is connected to the final classification or fully-connected layer for further processing.

2.5.6 Batch Normalization: In a deep neural network, this technique is applied to combat the internal covariate shift problem by normalizing the inputs of each layer. This technique has the power of stabilizing the learning process and can reduce the number of epochs to train a DNN (Peccia, 2018). To calculate normalized activations, this technique relies on the fowling formula (MathWorks. n.d.).

.

$$\hat{x}_i = \frac{x_i - \mu_B}{\sqrt{\sigma_B^2 + \epsilon}} \qquad 2.7$$

μ_B = mini-batch and every input channel's mean

σ^2_B = mini-batch and every input channel's variance

ϵ = numerical stabilization of parameters

2.5.7 Activation Function: The activation function is a node that helps to determine if the neuron will be triggered or not. Different types of activation functions exist. In this adopted architecture ReLU activation function was used. It is a popular activation function used in CNN. The biggest advantage of this function is that, it does not activate all neurons simultaneously; hence it is faster than other activation functions.

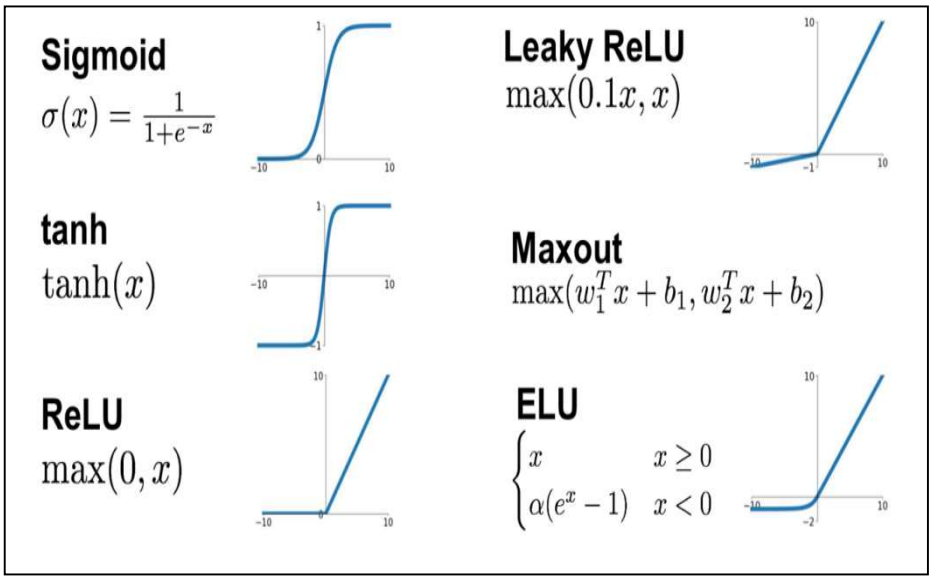

Figure 2.3: Different activation function (Source: Udofia, 2018).

2.6 Training

Generally, the training phase of CNN includes the forward propagation or forward pass, loss optimization, and back-propagation, etc. All these are discussed below.

2.6.1 Forward propagation: It refers to the process of calculating and storing intermediate variables from the input layer to the output layer accordingly, where inputs are fed through the neural network consisting of several convolutions, pooling, and fully connected layers (Dive into Deep Learning, n.d.).

2.6.2 Loss Optimization: Neural network outputs are tuned by changing the parameters' value such as weights, and the optimization is the function which carries out this task. There are several optimization algorithms for example; Root Mean Square Propagation (RMSProp), Adaptive Moment Estimation (Adam), Stochastic Gradient Descent (SGD) with momentum. Loss functions are helpful to train a neural network, and there are different types of loss function such as Regressive loss functions Classification loss functions, Embedding loss functions (Verma, 2019).

2.6.3 Back propagation: This is a technique of calculating the gradient of neural network parameters. More precisely, this method traverses the network in reverse order, from the end (output) to start (input) maintaining the chain rule from calculus (Dive into Deep Learning, n.d.).

2.6.4 Parameters and Hyper-parameters: In a model parameters refer to the features (such as weight and bias) that a model updates through forward and back-propagation. Whereas, hyper-parameters refer to the properties of the models that are fixed during the training phase. So, model parameters include the process of estimation that is done from the data automatically; whereas, hyper-parameters estimation is done manually to help the parameter`s estimation process (Brownlee, 2017). Based on role, we can divide the hyper-parameters into two categories: a) to determine the structure of a network (e. g. kernel size), b) to determine the training stage of a network (e. g. maximum epoch).

2.7 Modified Architecture Adopted in this Study

The selected model (**Figure 2.2**) was modified until getting the desired result. The major difference between the base model and the modified one is the pooling layer. There is no pooling layer in the modified model, and the reason is, instead of decreasing the representations' quantity to lessen the parameter's quantity and computations of the network, this study used the dropout layer directly. This technique not only helps in regularization (over the fitting problem) but also can stop the contribution of some randomly selected neurons temporarily; thus, it helps to reduce the computations in the network as well, and the process becomes faster. Besides, the modified model shows consistency in kernel size of the convolution layers.

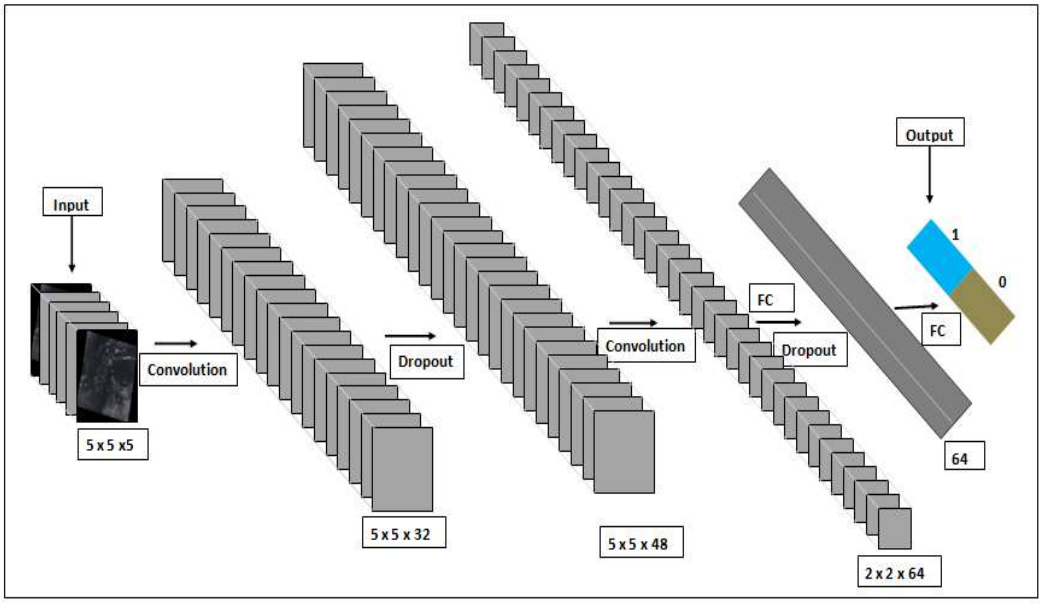

Figure 2.4: Modified CNN architecture adopted in this study

2.8 Artificial Neural Network

ANN is a highly powerful data processing tools. Till now, different types of Neural Networks (NNs) has been proposed, where the most common things are: the neurons, the link among the neurons, and the base algorithm for learning (Malik, 2005). ANN can be addressed as an interconnected group of nodes, like a network of neurons in a brain. So, it is a computational model inspired by animal's brains that are capable of pattern recognition. ANNs can be presented as interconnected neurons with the power of computing values from inputs by taking information through the network. The key benefit of the ANN is that the propagation of information in the neurons and the processing of information are conducted simultaneously (Udapa et al., 1997). An ANN is programmed through a learning method for a particular reason, for example; classification of data. When a specific component of the network collapses, its will continue without any difficulty. No doubt that ANN is gaining popularity for predicting the results about certain parameters. It can be applied for predicting response parameters from process parameters once trained properly (Mhatre et al., 2015).

2.9 ANN Architecture Adopted in the Study

Like a typical ANN architecture, this architecture also has three main stages, and those are a) input layer, b) hidden layer, and c) output layer. It should be mentioned that this architecture was adopted based on the Python environment used in MOLUSCE 3.0.13.

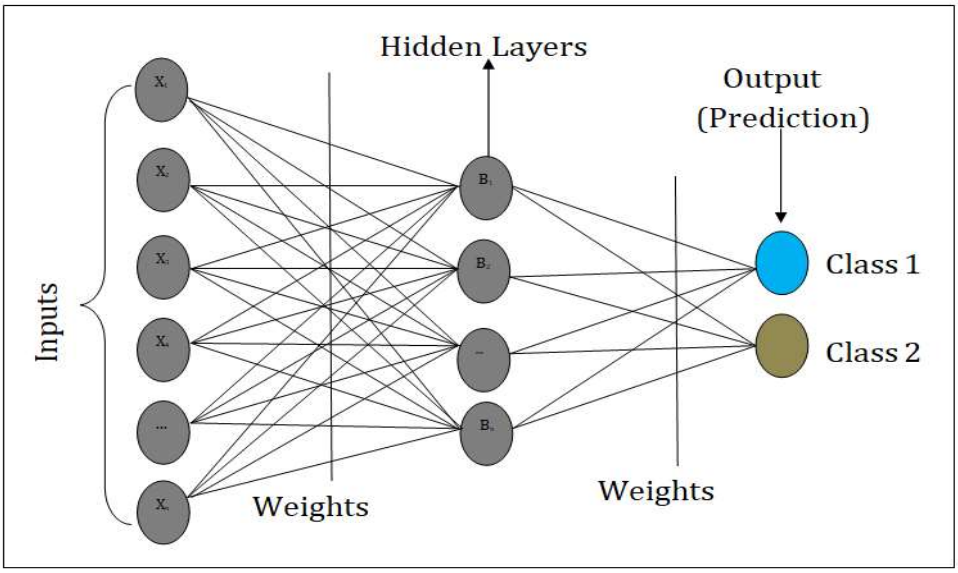

Figure 2.5: ANN skeleton adopted in this study

2.9.1 Input Layer: It receives input values of the attributes for each observation. The number of nodes in this layer equals the number explanatory variables.

2.9.2 Hidden Layer: Between the input and output layers, this layer is placed. In this layer, weights (values) are applied to the input and then transform those weighted values in a non-linear pattern through an activation function to the output. In a neural network, there may have one or more hidden layers.

2.9.3 Output Layer: This layer receives connections from hidden layers and responsible to produce the final outcome. In a neural network, there must have one output layer. To understand the whole process of the model, let's assume we have a satellite image of 800 pixels; so, we will have 800 neurons in the input layer. These neurons will be connected to the next layer (hidden layer) through the channels. Each channel has a numerical value known as weight. Inputs of the first layer are multiplied to the corresponding weight, and their sum is transferred to the hidden layer as input, where each neuron is associated with a value called bias. This bias is then added to the input sum. This entire process can be expressed as;

$$(X_1 \cdot W_1 + X_2 \cdot W_2 + \dots \dots . + X_n . W_n) + B1 \qquad 2.8$$

Here,
X= value of the neurons in the input layer
W= weighted value
B= bias value

These neurons then send the data to the next layer through an activation function over the channel. This process is known as forwarding propagation In this case, in the output layer, the neuron with the highest value predicts the result, and this result is nothing but the probability. As we know, a neural network may predict wrong a backward propagation works to adjust the weights. So in most cases, these forward and backward propagations work as a cycle until the network can predict most of the results correctly.

CHAPTER THREE
Study Area Profile and Used Datasets

3.1 Introduction

3.2 Study Area Profile

3.3 Datasets Utilized

3.3.1 Landsat-5

3.3.2 Landsat-8

3.3.3 Other Data Sets

3.1 Introduction

This chapter is representing the discussion about the selected study area, like the location and some features of the study area. Besides, a description of the used dataset with collection sources has also been shown here.

3.2 Study Area Profile

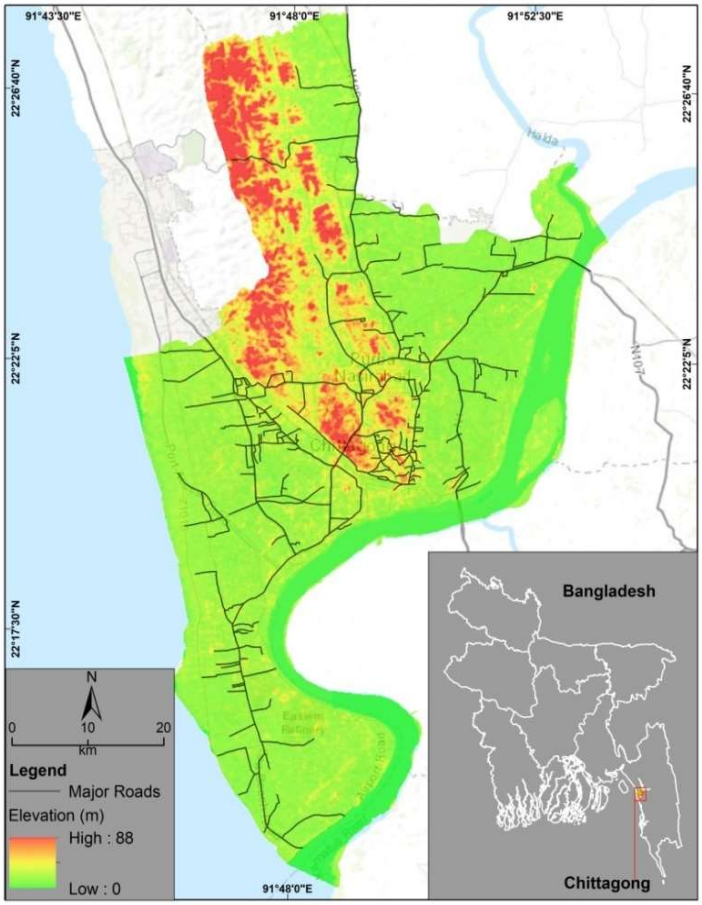

Figure 3.1: Study area's absolute location

Chittagong City is situated in the southeastern edge of Bangladesh. The absolute location of the city is 22.13° and 22.28° north to 91.45° and 91.54° east (Ahmed and Dewan, 2017). There has a tropical monsoon climate in this region, with hot and humid summers and slightly cold winters. The summer's maximum temperature is 32.3 °C, while the winter's minimum temperature is 13 °C. Annual rainfall in this area, on the other hand, ranges from 2400 to 3000 mm (BMD, 2013; Hassan and Nazem, 2015). As the second-largest metropolitan city in Bangladesh, Chittagong is a commercially very important city (Roy and Saha, 2016). It is known as the city for

export and import. The prime position of the port has made it an important economic center, attracting massive influx of foreign investment into garment industry, ship breaking industry, and oil refinery operations. (Hussain et al., 2016). The city owns 40 percent of the large-scale industries of the country (BBS, 2013).

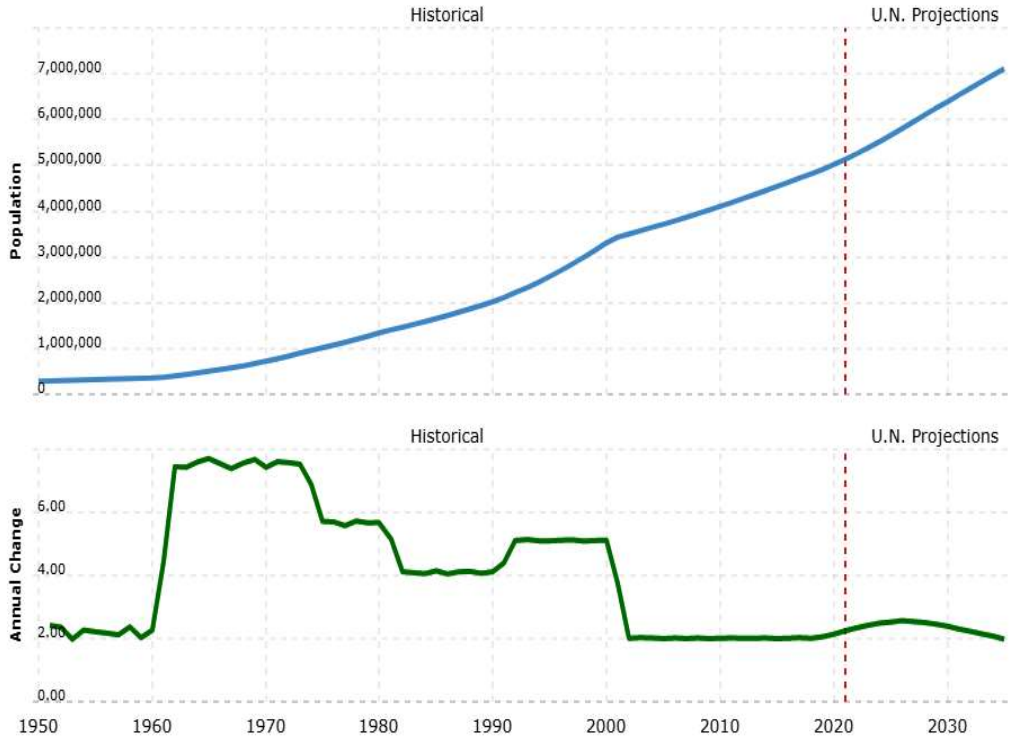

Figure 3.2: Population in Chittagong metropolitan area (Source: Macrotrends LLC, n.d.)

At the national level, it shares 19.7 percent of the urban population with 30 percent of the GDP (BBS 2011). Chittagong is also a biodiversity hotspot at the crossroads of several bio-geographical divisions (Islam, 2009). Recently, land-use alterations have put the city under the stress of experiencing numerous economic, societal, and environmental problems (Hussain et al., 2016), where the water-related problem is one of the common ones.

3.3 Datasets Utilized

Including vector and raster data, different datasets were used in this study. All of them are presented below.

3.3.1 Landsat-5: With the MSS and TM sensors, this mission was launched on March 1, 1984. Before decommissioned on June 5, 2013, it set a Guinness World Record by providing earth imagining data for 29 years (USGS, n.d.).

In 1992 and 1999, respectively, the procurement of Landsat 5 MSS data for the US and worldwide was halted. From June 2012 to January 2013, restricted acquisitions were reported (Earth Observation System. n.d.).

Table 3.1: Landsat 5 (MSS) band`s properties

Band	Specification	Wavelength (µm)	Spatial Resolution (m)
1	Visible Green	0.5 - 0.6	60
2	Visible Red	0.6 - 0.7	60
3	NIR	0.7 - 0.8	60
4	NIR	0.8 - 1.1	60

On Landsat 4 and Landsat 5, the Landsat TM sensor was adjusted to create images consisting of seven bands. (6 spectral bands and 1 thermal band) (Earth Observation System. n.d.).

Table 3.2: Landsat 5 (TM) band`s properties

Band	Specification	Wavelength (µm)	Spatial Resolution (m)
1	Visible Blue	0.45 - 0.52	30
2	Visible Green	0.52 - 0.60	30
3	Visible Red	0.63 - 0.69	30
4	NIR	0.76 - 0.90	30
5	SWIR 1	1.55 - 1.75	30
6	Thermal	10.40 - 12.50	120
7	SWIR 2	2.08 - 2.35	30

3.3.2 Landsat-8: Landsat 8 mission was incorporated on February 11, 2013 with the OLI and TIRS Sensor instruments (USGS. n.d.). TIRS collects images with 100 m spatial resolution. The key purposes of this sensor are to obtain the attributes of surface temperature and to examine the heat and humidity transfer methods industries, such as agriculture and water management. The main advantage of both TIRS and OLI instruments is that they can scan along the spacecraft track; hence, the radiometric distortions less occur than the transverse scanning instruments of previous Landsat satellites (Earth Observation System. n.d.).

Table 3.3: Landsat 8 band`s properties

Band	Specification	Wavelength (µm)	Spatial Resolution (m)
1	Coastal	0.43 - 0.45	30
2	Blue	0.45 - 0.51	30
3	Green	0.53 - 0.59	30
4	Red	0.63 - 0.67	30
5	NIR	0.85 - 0.88	30
6	SWIR 1	1.57 - 1.65	30
7	SWIR 2	2.11 - 2.29	30
8	Pan	0.50 - 0.68	15
9	Cirrus	1.36 - 1.38	30
10	TIRS 1	10.60 - 11.19	30 (100)
11	TIRS 2	11.50 - 12.51	30 (100)

3.3.3 Other Data Sets: Apart from satellite image, some auxiliary data also used in this study, which are

a. Major road network
b. Rainfall
c. Temperature
d. DEM (ASTER)
e. Ground truth data

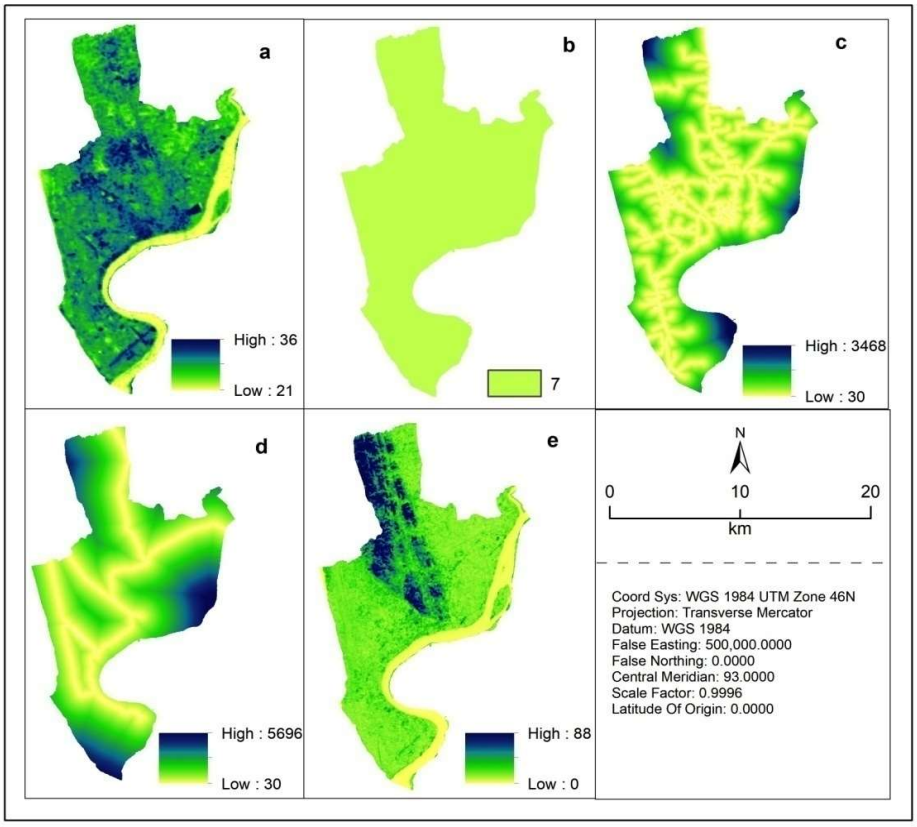

Figure 3.3: Different variables used in this study a) temperature, b) rainfall, c) distance to road, d) distance to railway, and e) DEM

Here, a short description of the temperature data, DEM and ground truth data is discussed in detail.

Capturing Temperature Data: Temperature is one of the main auxiliary data or variables in this study. To extract this temperature data, remotely sensed thermal bands were used. At first, to convert image values from DN to radiance following two equations were applied respectively (USGS, n.d.).

$$L_\lambda = \left(\frac{LMAX_\lambda - LMIN_\lambda}{QCALMAX - QCALMIN}\right) * (QCAL - QCALMIN) + LMIN_\lambda \quad 3.1$$

Here:
L_λ = Sensor aperture's spectral radiance
QCAL = DN value of quantized calibrated pixel
$LMIN_\lambda$ = Scaled spectral radiance in terms of QCALMIN
$LMAX_\lambda$ = Scaled spectral radiance in terms of QCALMAX
QCALMIN = Value of mini quantized calibrated pixel
QCALMAX = Value of max quantized calibrated pixel value

$$L_\lambda = ML * Q_{cal} + A_L \quad 3.2$$

L_λ = Spectral radiance
ML = Multiplicative scaling factor
A_L = Additive scaling factor
Q_{cal} = Value of pixel at level 1 (DN)

After that, to convert the outputs of the previous two equations into temperature (Kelvin) following formula was applied.

$$T = \frac{K2}{ln\left(\frac{K1}{L_\lambda}\right)} + 1 \quad 3.3$$

T = Brightness temperature at the top of the atmosphere
L_λ = Spectral radiance At the top of the atmosphere
K1 = Constant value for band-specific thermal conversion
K2 = Constant value for band-specific thermal conversion constant

Finally, the extracted temperature data was converted to degree Celsius by subtracting 273.15 from the outputs.

DEM (ASTER): The first ASTER edition was published in June 2009. It was created using stereo-pair images captured by the ASTER instrument (Jet Propulsion Laboratory. n.d.). Coverage of ASTER GDEM extends from 83 ° n to 83 ° s latitude, with 99 percent of the landmass of Earth. In 2019 ASTER GDEM-iii was released, which includes additional stereo-pairs. To increase accuracy (both horizontal and vertical) and spatial resolution refined production algorithm was applied. Moreover, the GeoTIFF format and the same tile structure as V1 and V22 are available in the ASTER GDEM V3 (Jet Propulsion Laboratory. n.d.). Considering the updated facilities, in this study, ASTER GDEM V3 was used.

Ground Truth Data: To check the accuracy of the outputs, ground truth data were collected from different sources. Most of these data were prepared by other researchers to carry out different scientific studies.These data required some pr-processing. In this study, all types of water features were categorized as the water body in general, but in-ground truth data, there were open water bodies, surface water bodies, lowlands, etc. So, to compare with the outputs of this study, all the water features were merged into a single class.

Table 3.4: Different datasets used in this study

Serial	Specification	Types	Resolution (m)	Sources
1	Landsat 5 & 8	Raster	30	USGS
2	Temperature	Raster	30	Landsat 5 & 8
3	Rainfall	Excel	-	BMD
4	Major Roads	Vector	-	GPAD
5	Railway	Vector	-	GPAD
6	DEM	Raster	30	NASA Earth data
7	Ground truth Data	Vector	-	Different sources

CHAPTER FOUR
Methodological Workflow

4.1 Introduction

4.2 Before Data analysis

4.3 During Data Analysis

4.4 After Data Analysis

4.1 Introduction

This chapter is discussing about the whole methodological flow of the study. For analytical purposes, the study workflow can be divided as a) before data analysis, b) during data analysis, and c) after data analysis. All these three phases are presented below with appropriate discussion.

4.2 Before Data analysis

Literature Review and Identifying Research Goals: The study started with a literature survey focusing on the research theme i.e. urban water bodies and deep learning. Based on the literature survey, some research goals (objectives) were set as the basement of the study. These objectives have not only fulfilled the research gap but also help to step forward to study urban water bodies using modern technologies like deep learning.

Data Collection: The major data of this study was satellite imagery. All the satellite images were collected from the USGS Earth Explorer website. Data were captured for the years 1996 (for training and testing the CNN model), 2000, 2005,2010,2015, and 2020 (for identifying spatio-temporal changes in water bodies). Depending on the seasonal variation, the water level in natural reservoirs varies in Bangladesh; therefor, February was considered as the most suitable month to study urban water bodies, As the water level in this month is more stable than in others. Besides, some auxiliary data also collected from different sources.

Data pre-processing: Under the data pre-processing section following tasks were done

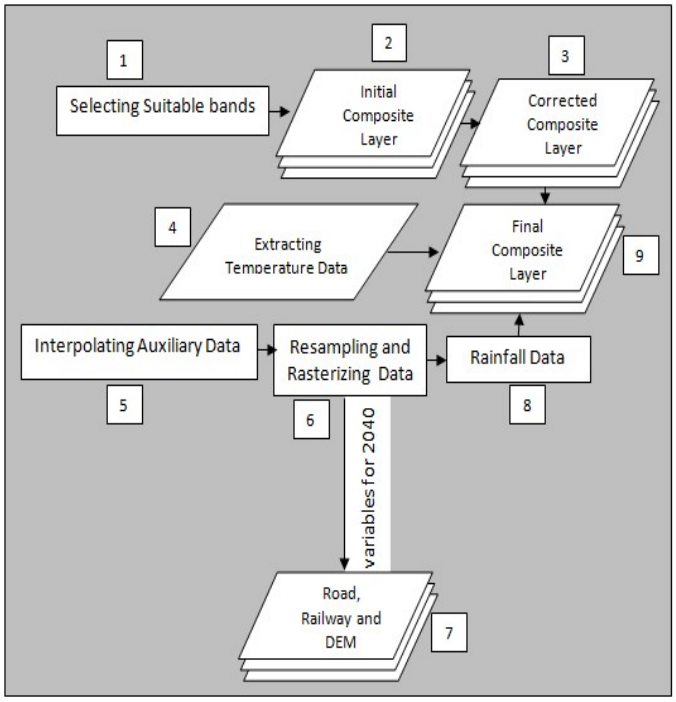

Figure 4.1: Steps followed in image processing and data preparation

Initial Layer stacking: Initial band combination or layer stacking was done using three bands (band 6,5,1 for Landsat 8 and 5,4,3 for Landsat 5). Here, a question may arise, why this band combination was selected? The answer is simple as the question. Even though this band combination is suitable for vegetation health monitoring, the water features are also very vibrant than in other band combinations. The reason can be better understood by looking at the **Figure 4.2**, which is following the same band combination (5,4,3).

Image Correction: Here two types of radiometric corrections were done to all initially stacked layers, those are haze reduction and noise reduction. The purpose of these corrections was to improve the interpretability and the quality of the data. The radiation observed by the sensor may be impacted by different factors like solar azimuth; thus, satellite recorded energy may differ from the original energy transmitted from the surface. To overlook this problem or to achieve the true ground radiance or reflectance values, radiometric correction is very effective (Humboldt State University, 2013).

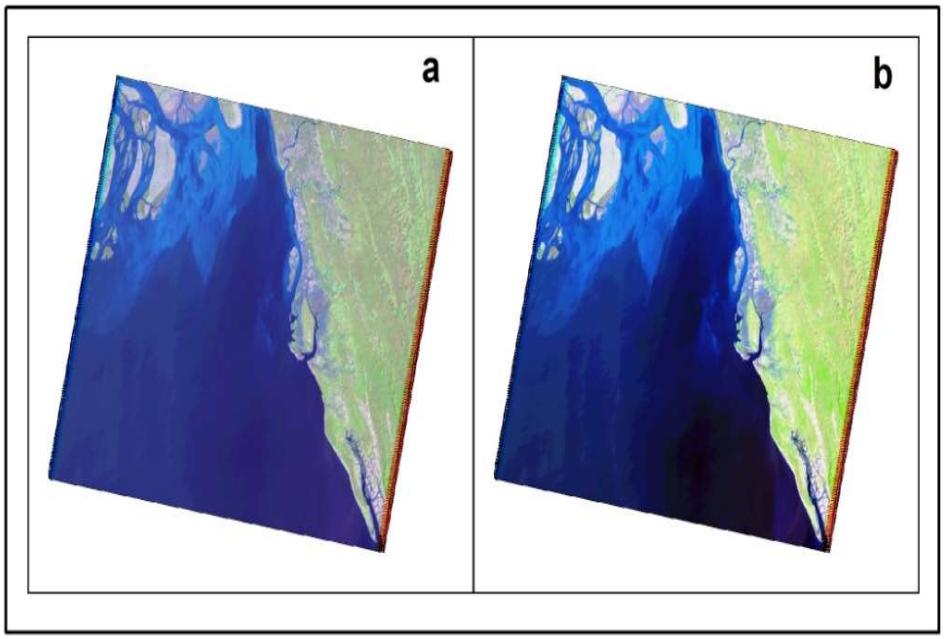

Figure 4.2: Result of image pre-processing a) before image correction, b) after image correction

Preparing Other Data: Apart from satellite imagery, other data like major roads, railway, elevation, temperature, and rainfall data were prepared depending on the nature of the data and the technique required to process those data. For example, to maintain the extent of the data (columns, rows=518,912 and cell size=30 x30), we need an equal number of cells in each raster, and for this, the Kriging interpolation method was applied. To calculate the missing or unmeasured value, this method weights the existing or measured values based on the search radius defined by the user.

The formula of this method can be expressed as follow (ArcGIS for Desktop n.d.):

$$z^*(x_0) = \sum_{i=1}^{N} \lambda_i z(x_i) \qquad 4.1$$

Here:
z * (x0) = Calculated value at x0;
z(xi) = Observed values at xi;
N = Size of the sample
λi = Weights for xi

In this study Universal Krignig Model was applied, mathematically which can be shown as follow (ArcGIS for Desktop n.d.):

$$Z(s) = \mu(s) + \varepsilon(s) \quad 4.2$$

Where,
$\mu(s)$=deterministic component
$\varepsilon(s)$=stochastic component

Preparing Final Composite Image: All the final campsite layer were consist of 5 bands, where first 3 bands were satellite images (band 6,5,1 for Landsat 8 and 5,4,3 for Landsat 5), and the other two were processed raster (temperature and rainfall).

4.3 During Data Analysis

This phase mainly includes the adoption of the architectures. As it is mentioned earlier in this study, mainly two architectures (CNN and ANN) were adopted which are shown in (Chapter Two); however, this study modified the CNN architecture. The modified version of the architecture is **Figure 2.4.**

4.3.1 Adopting the CNN Architecture

4.3.1.1 Training the Network: The prediction level of a network largely depends on the input dataset. For training and testing purposes, we used 2-dimensional composite image (5 bands) and corresponding water body binary layer. The binary layer was created from ground-truth data. Both composite image and binary image were used to produce training and testing dataset based on 5 x 5 kernel or window size; thus, we got 18643 image chips. Following the tradition, the data was divided into two parts, training data, and testing data. This training and testing split is done to evaluate the performance of a model. Here, the training and testing proportion are 80:20. More specifically, 80% of the data was used for training the network and 20% for validating or testing the network.

To train the classification network image chips and corresponding ground-truth binary were used as the input. A model may produce outputs with a negative value or greater than one to overlook this problem a softmax function was used. This function identifies probability distributions in the potential outcomes. Following that, log loss was calculated with the help of ground-truth labels. The log loss function predicts the output of a classification model with a value varying from 0 to1. When prediction

likelihood diverges from the ground-truth data, the log loss value becomes high. Based on a backward propagation process, this log loss calculation is then used to update the network with the help of Stochastic Gradient Descent with momentum.

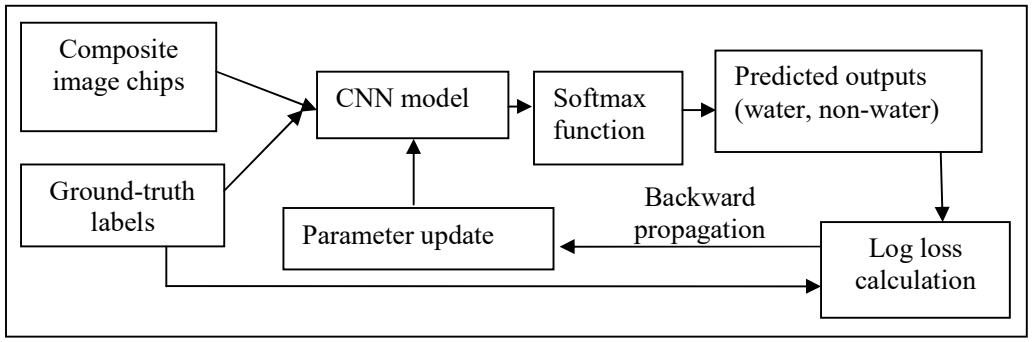

Figure 4.3: Stages followed in training the classification network.

4.3.1.2 Experimental Settings: Based on Python 3.0 environment, the experiment was run on a server which has Intel® Core ™ i7-1165G7 Processor, 16 GB DDR-4 RAM, 512 GB PCIe® NVMe ™ M.2 SSD Hard Drive, and NVIDIA® GeForce® MX450 Graphics.

For training and testing purposes, we used 1996 data, but we did not consider that output (water bodies in 1996) for change detection. Using the model, we tried to show the changes from the 2000 to 2020 lassification result.

One of the most common problems of a neural network is failing to memorize the training data; consequently, a network produces poor predictions or outputs. This situation is commonly known as an over-fitting problem. To adopt our model with this problem, we used post-training validation with the test data.

The model was trained using Stochastic Gradient Descent with momentum where the hyperparameter, like momentum were fixed 0.9. Other parameters are shown in Table. To set these parameters we followed the study conducted by Zhang et al., (2018).

Epoch: In a neural network, epoch refers to a process by which the entire dataset is passed through the forward and backward to complete a cycle. A neural network usually needs more than a few epochs to be trained. In this study, the maximum number of the epoch was terminated to 25.

Learning Rate: It is a changeable hyperparameter having a small positive value (ranged from 0.00 to1.0). This learning rate determines the speed of a model's adaptation to the problem. In this study, the learning rate was fixed to 0.1.

Mini-batch size: It can be defined as the variant of gradient descent algorithm that can divide training datasets into several small batches. These small batches then can be used for calculating the error and coefficient value of the model. In this study, the tested mini-batch was fixed to 100.

Table 4.1: Hyper-parameter set for the CNN model

Hyper-parameters	**Values**
Epochs -Limit	25
Momentum	0.9
Weight Decay/L2 Regularization	0.00005
Learning Rate	0.1
Mini-batch Size	100

It should be noted, based on the mentioned experimental setting, the only experiment that we have conducted here focused on the classification of Landsat images (with or without auxiliary data) to detect the changes in water bodies.

4.3.1.3 Network Performance Evaluation: Model performance was assessed based on the overall accuracy technique. Generally, overall accuracy is calculated based on the following formula (Google Developers n.d.):

$$OA = \frac{Number\ of\ correct\ predictions}{Total\ number\ of\ predictions} \quad 4.3$$

But for binary classification, accuracy can be assessed in terms of positive and negative predictions as follow (Google Developers n.d.):

$$OA = \frac{TP + TN}{TP + TN + FP + FN} \quad 4.4$$

Here, TP = True Positives, TN = True Negatives, FP = False Positives, and FN = False Negatives.

Assessing the Influence of Auxiliary Data: Apart from spectral bands, our input image had two processed raster or auxiliary data (temperature and rainfall). To identify the influence of auxiliary data on model performance or classification outputs, we had to test the model with and without auxiliary data. In this case, input data without auxiliary data produced output with a bit higher accuracy than with auxiliary data. Therefore, in the final classification, we used composite images without auxiliary data as input.

4.3.1.4 Post-classification Accuracy Assessment: As the accuracy level at the testing stage was satisfactory, we considered the architecture fit with the best hyperparameter and was selected for final classification. The final classification outputs were assessed both quantitatively and qualitatively.

Quantitative Accuracy Assessment: The quantitative assessment was done using precision and recall and F1 score calculation. Descriptions of these calculations are given below.

Precision: It refers to the ratio between the number of correctly classified positive samples to the total number of positive samples (either correctly or incorrectly). The degree of precision is high when the model maximizes the true positive classification and minimizes the false positive classification. The equation to calculate precision level is as follow (Brownlee, 2020):

$$Precision = \frac{truePositives}{truePositives + falsePositives} \quad 4.5$$

Recall: It can be defined as the ratio between the number of positive samples correctly classified as positive to the total number of observations. The recall is concerned with how the positive samples are classified. The higher recall value means more positive samples detected. Recall can be classified using the following formula (Brownlee, 2020:

$$Recall = \frac{truePositives}{truePositives + falseNegatives} \quad 4.6$$

F1 score: The F1-score is calculated based on the combination of the model's accuracy and recall, and it considers both false positive and false negative values (Brownlee, 2020).

$$F1 = 2 \times \frac{precision \times recall}{precision + recall} \quad 4.7$$

Qualitative Accuracy Assessment: Post-classification qualitative assessment was done using the swipe and flicker tool in ArcGIS. By overlaying the ground-truth labels, these tools allow the visual interpretation of the classification results.

4.3.2 Adopting the ANN Architecture: Before simulating water bodies for 2040, the model was validated by producing output for 2020 using classified data (water and non-water data) for 2000 and 2010. Besides classified water and non-water data, some variables like DEM, road network, and railway data were also utilized. To predict the outputs for 2020, different parameters were fixed, which are shown in **Table 4.2.**

Table 4.2 : Parameters set to configure ANN model

Parameters	**Value**
Window size	5x5
Learning rate	0.10
Maximum iteration	1000
Hidden layers	10
Momentum	0.05

At the validation stage, the overall accuracy level was about 97%. Since this accuracy level was high, the model was considered the best fit for simulating output for 2040.

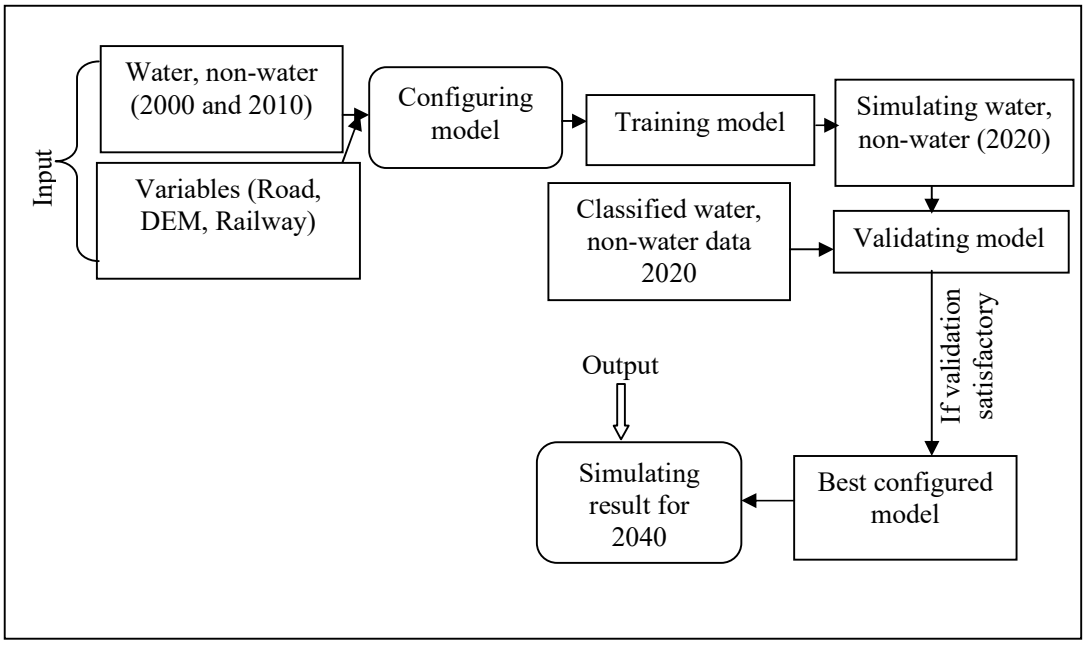

Figure 4.4: Methodological workflow of simulating water bodies for 2040

4.4 After Data Analysis

4.4.1 Change Detection: This part was done in ArcGIS. To understand the change detection process, let's assume we have classified images for 2000 and 2005. We want to identify the changes in water bodies within these five years. First, we need to intersect both images. In the intersected image, we will get the classified data (water, non-water) for both 2000 and 2005 in different columns. Let's think data column for 2000 = classified_00 and for 2005= classified_05. Now, we need to make a new column to identify the transition between these two columns (2000 and 2005). Using field calculator's python environment, we can run the following code: *"classified_00"+ "to"+ classified_05"*. This simple code will fill the new column by combining both classified_00 and classified_05 data (e.g. non-water to water). Using this newly generated data column, we can easily identify the changes in both water and non-water bodies and can also calculate the quantity of transited area.

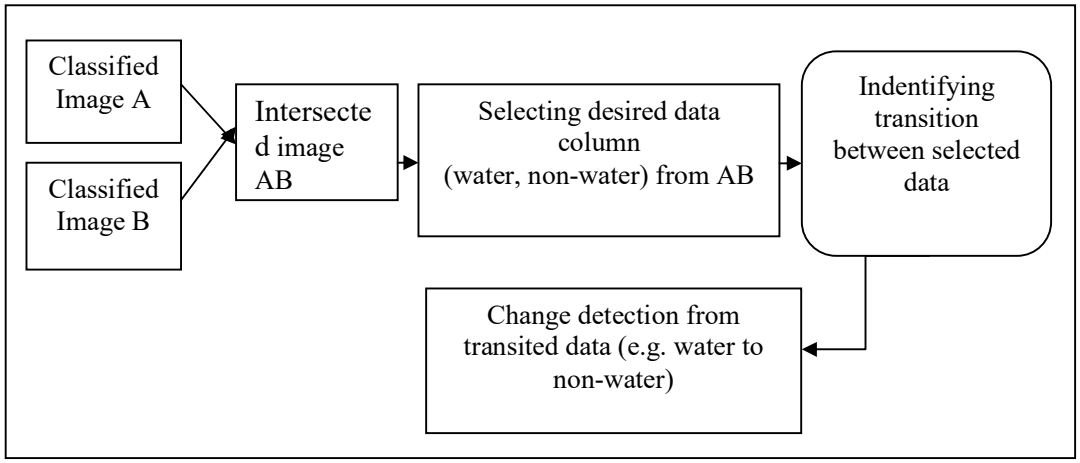

Figure 4.5: Methodology followed in change detection

4.4.2 Data Visualization: After change detection, all the findings were visualized with necessary tables, charts, and maps using data presentation platforms like ArcGIS 10.3, Tableau 19.4.368.0, and Microsoft Word and Excel 2007.

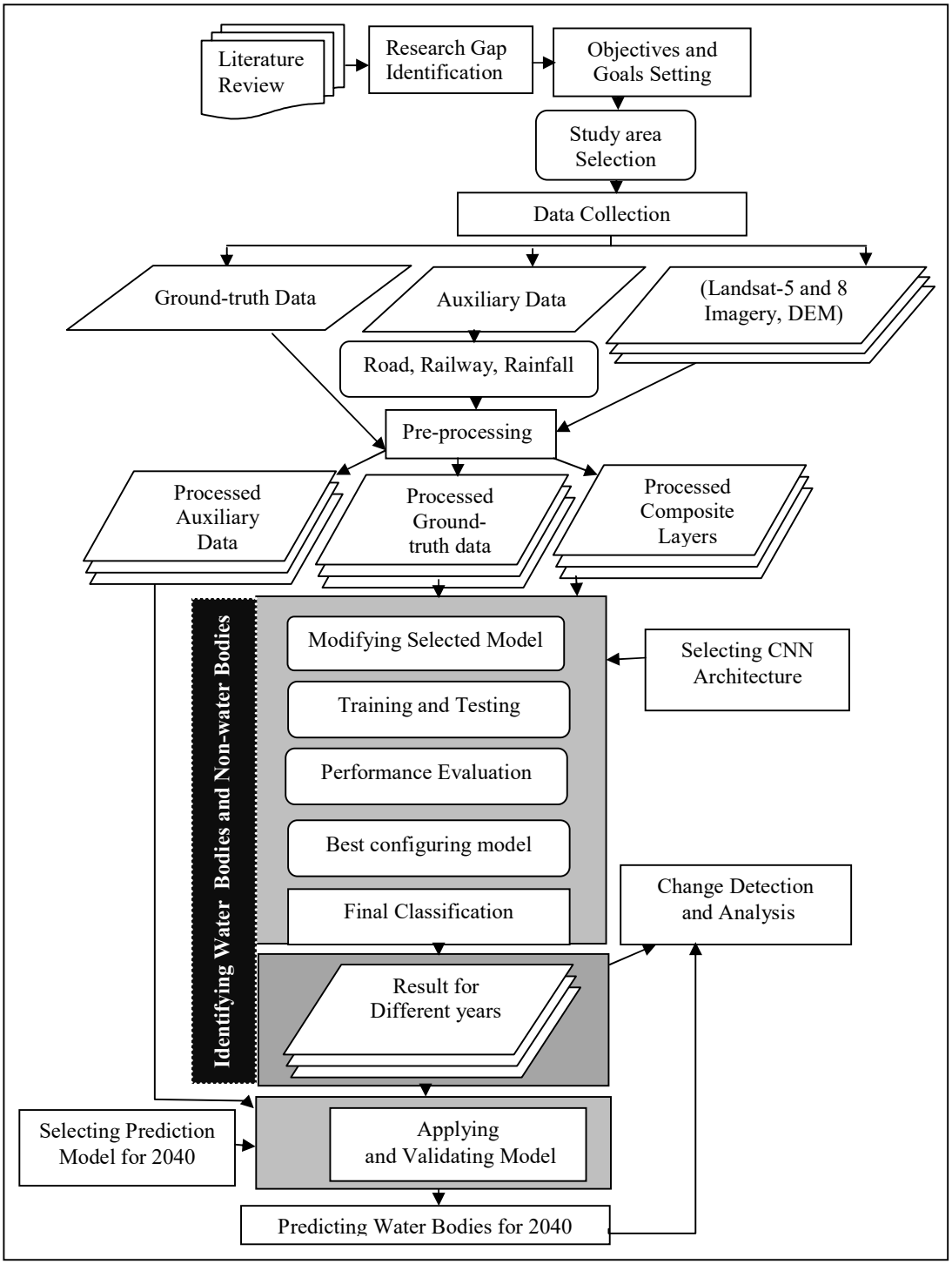

Figure 4.6: Methodological work flow of the study at glance

CHAPTER FIVE
Results and Discussion

5.1 Introduction

5.2 Performance Evaluation and Classification Results

5.2.1 Influence of Auxiliary Data

5.2.2 Post-classification Accuracy with Different Kernel Size

5.2.3 Classification Outputs (Water and Non-water bodies)

5.3 Post-classification Change Detection (2000 -2020)

5.4 Water and Non-water Simulation for 2040

5.1 Introduction

This chapter is showing the findings of the study including the performance and outputs of the model (water and non-water bodies in different years), changes in water and non-water bodies from 2000 to 2020, the simulation of the water non-water for 2040, and interaction between water and non-water from 2020 to 2040.

5.2 Performance Evaluation and Classification Results

5.2.1 Influence of Auxiliary Data: Auxiliary data might influence the accuracy level of the model. From this belief, the model was also tested with only three spectral bands (band 6,5,1 for Landsat 8 and 5,4,3 for Landsat 5). The result revealed that the auxiliary data have some influence on the accuracy level of the model. The model can predict the result with 93% accuracy without any auxiliary data, but with auxiliary data, this percentage is slightly lower (92.28%), as shown in **Figure 5.1**. For this reason, to find out the changes in water bodies from 2000 to 2040, we relied on the composite image without auxiliary data.

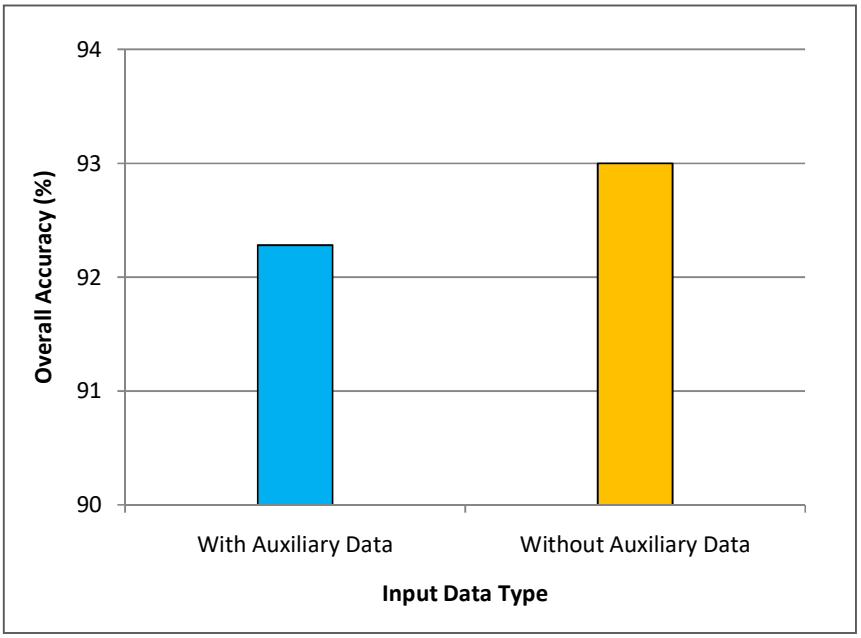

Figure 5.1 : Influence of auxiliary data on model performance

5.2.2 Accuracy with Different Kernel Size: Although the results discussed in this chapter based on kernel size 3 x 3, the model applied in this study was tested with different kernel sizes. The other two kernels were 5 x 5 and 7 x 7.

Table 5.1: Accuracy level of CNN model for different years

Time	Kernel Size	Precision	Recall	F1
2000	3 x 3	0.90	0.94	0.92
	5 x 5	0.88	0.90	0.89
	7 x 7	0.85	0.90	0.86
2005	3 x 3	0.90	0.94	0.91
	5 x 5	0.88	0.90	0.89
	7 x 7	0.85	0.90	0.86
2010	3 x 3	0.93	0.94	0.94
	5 x 5	0.87	0.90	0.89
	7 x 7	0.86	0.92	0.89
2015	3 x 3	0.92	0.95	0.94
	5 x 5	0.87	0.88	0.88
	7 x 7	0.86	0.92	0.89
2020	3 x 3	0.93	0.94	0.93
	5 x 5	0.89	0.92	0.90
	7 x 7	0.88	0.92	0.90

So, a question may arise why 3 x 3 kernel was selected to explore the Spatio-temporal changes in urban water bodies?

Looking at the **Figure 5.2**, we can easily understand, in all three categories (precision, recall, and F1), 3x3 kernel produced the most accurate result for all the years. The accuracy level of the prediction was ≥ 0.9. For example, for the year 2010, the precision, recall, and F1 scores with kernel 3x3 were 0.93, 0.94, and 0.94 accordingly. In that year, these scores with kernel 5x5 were 0.87, 0.90, and 0.89, respectively. From the graphical comparison, we can say, to extract information for mid to low-resolution satellite imagery, 3 x 3 kernel would be the best choice.

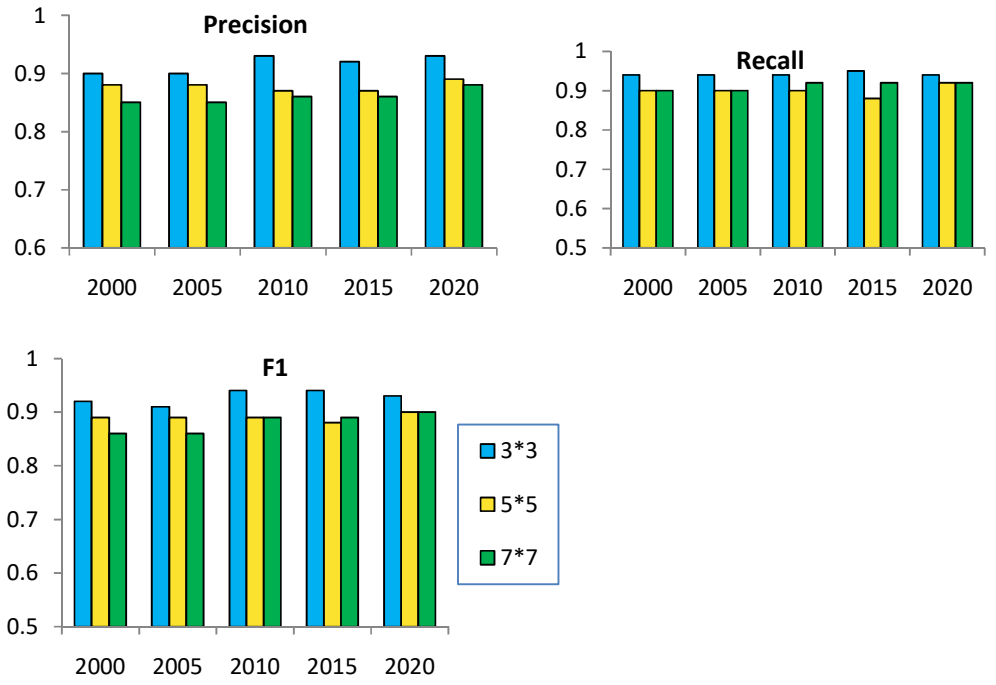

Figure 5.2: Performance of the model with different kernel sizes

5.2.3 Classification Outputs (Water and Non-water bodies): Analysis of this section has been done based on the outputs of the CNN model for different years.

Looking at the results, we can see, water bodies in Chittagong did not experience major changes between 2000 and 2020, but some changes are noticeable each year.

Table 5.2: Area coverage of water and non-water bodies in the selected time frame.

Year	Water bodies (sq. km)	Non-water bodies (sq. km)	Total Area (sq. km)
2000	27.498	168.582	196.080
2005	28.561	167.519	196.080
2010	29.468	166.611	196.080
2015	28.877	167.203	196.080
2020	26.389	169.691	196.080

During the study period, non-water bodies were always higher than that of water bodies. The lowest non-water bodies (166.611 sq km) and the highest water bodies (29.468 sq km) were in 2010. On the other hand, the highest non-water bodies were recorded (169.691 sq km) in 2010, when water bodies were 26.389 sq km.

In 2000 and 2005, water bodies in the same place were between 27 to 28 sq km, but in 2015 the figure was around 29 sq km. Similarly, non-water bodies in the years were around 167 to 168 sq km.

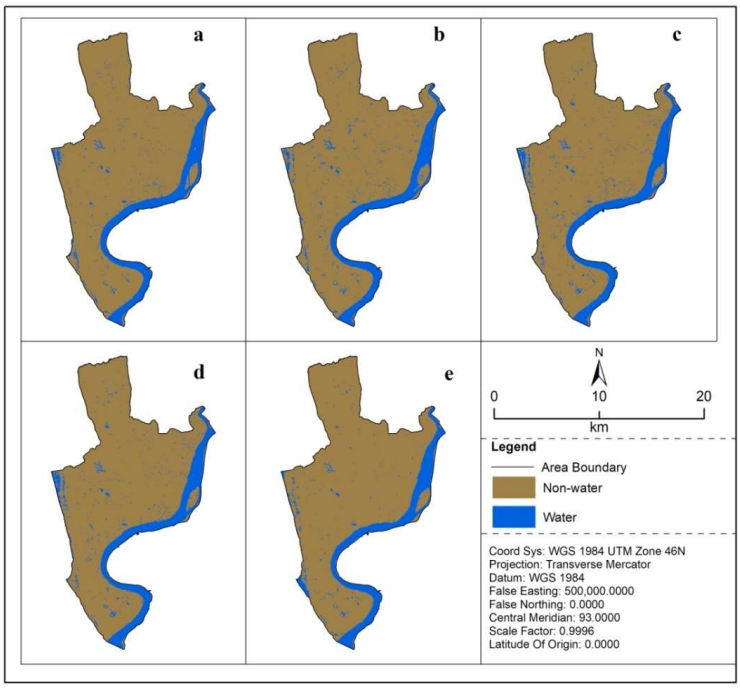

Figure 5.3: Water and non-water bodies in Chittagong (2000 - 2020)
a) 2000, b) 2005, c) 2010, d) 2015, and e) 2020

Figure 5.4 is showing the percentage of area coverage by water and non-water landscapes in different years. It is understandable from the figure water bodies were much less than non-water bodies in all the selected years. Although there was a hint of a slight increment in water bodies from 2000 to 2010, this increment was only in open water bodies i.e. inland water bodies did not experience dramatic change.

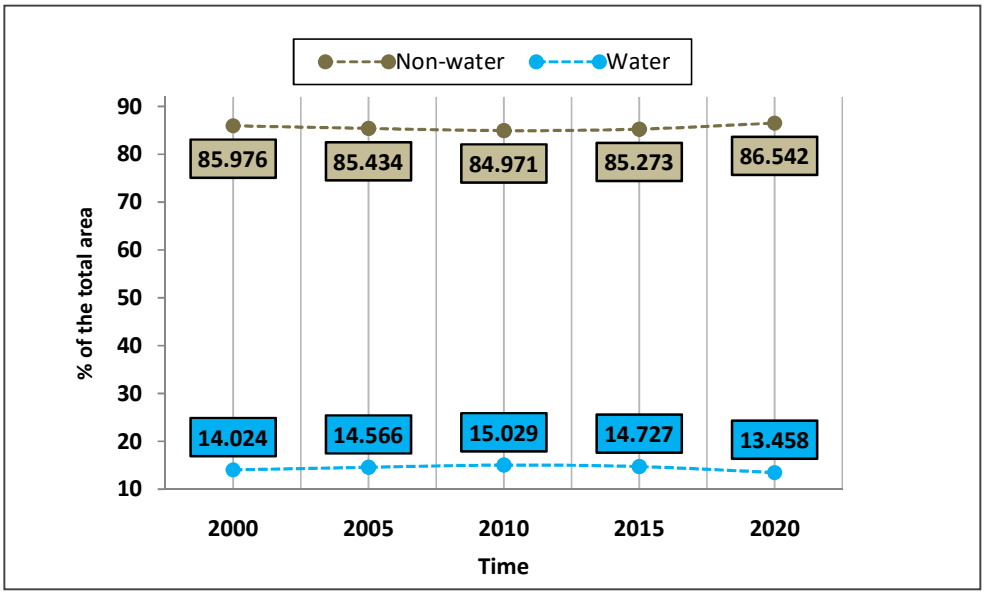

Figure 5.4: Percentage-wise area coverage of water and non-water bodies (2000 - 2020)

5.3 Post-classification Change Detection (2000 -2020)

Now based on water non-water interaction, we will try to see at what rate these water bodies had changed and where those changes took place. If we look at the overall scenario (2000 to 2020), we can see that water bodies have increased by about 1.00 sq km from 2000 to 2010. On the other hand, between 2010 and 2015, water bodies decreased by about 0.60 sq km. Similarly, from 2015 to 2020, about 2.5 sq km of water bodies were replaced by other land covers.

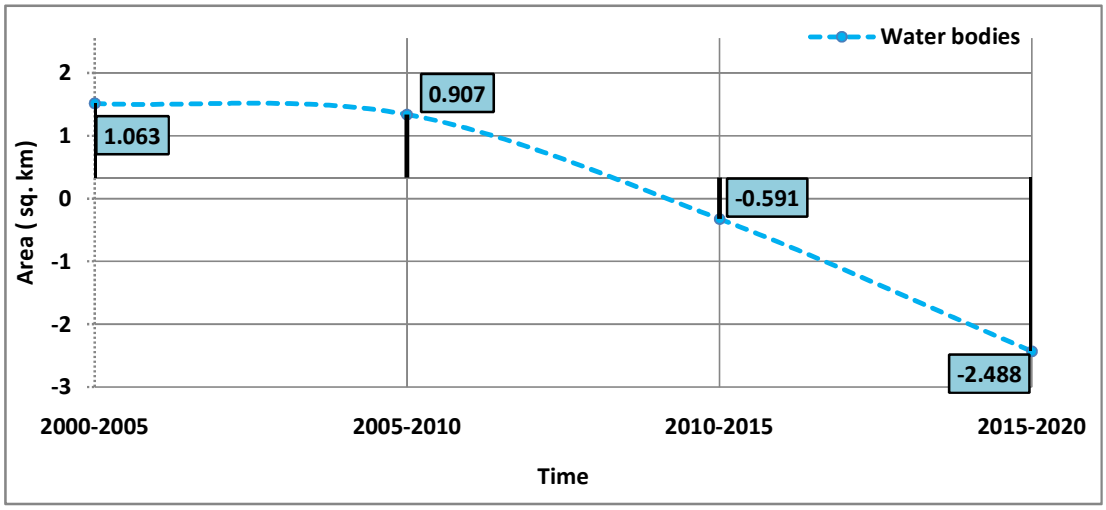

Figure 5.5: Trend of changes in urban water bodies in Chittagong city (2000 - 2020)

Moving on to the interaction between water bodies and non-water bodies from 2000 to 2005, we can see there was no change in the 164,780 sq km non-water bodies within these five years, the same result recorded for 24,799 sq km water bodies. During this period, 3.780 sq km non- water bodies converted to water bodies and 2.721 sq km of water bodies changed to non-water bodies.

Table 5.3: Quantitative Interaction between water and non-water (2000- 2020)

Time	2000-2005	2005-2010	2010-2015	2015-2020
Non-water	164.780	163.281	165.694	164.792
Non-water to Water	3.780	4.237	2.046	2.345
Water to Non-water	2.721	3.341	2.637	4.904
Water	24.799	25.220	25.703	24.039
Total Area (sq km)	196.080	196.080	196.080	196.080

The picture of the interaction from 2005 to 2010 depicts, like previous 5 years, there had no change in 163.281 sq km of non-water bodies and 25.220 sq km of water bodies. The rate of transition from non-water bodies to water bodies was a little higher than the previous phase, which was 2.161 %of the total area. The percentage of water bodies to non-water bodies was 1.704 % of the study area.

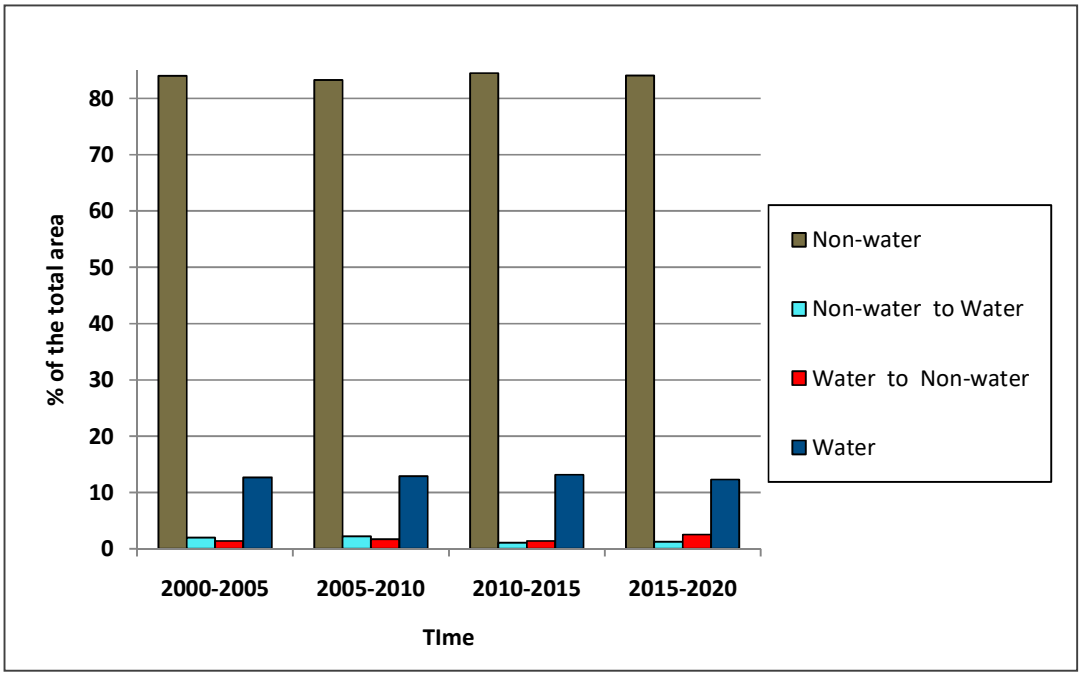

Figure 5.6: Comparison of water non-water interaction for different years

Five years later (2010 to 2015), almost the same quantity of water bodies and non-water bodies exchanged area. That means, the quantity of change from water bodies to non-water bodies and non-water bodies to water bodies at this time was almost similar. The figure was 1 to 1. 345% of the study area and in number which was 2 to 2. 637 sq km.

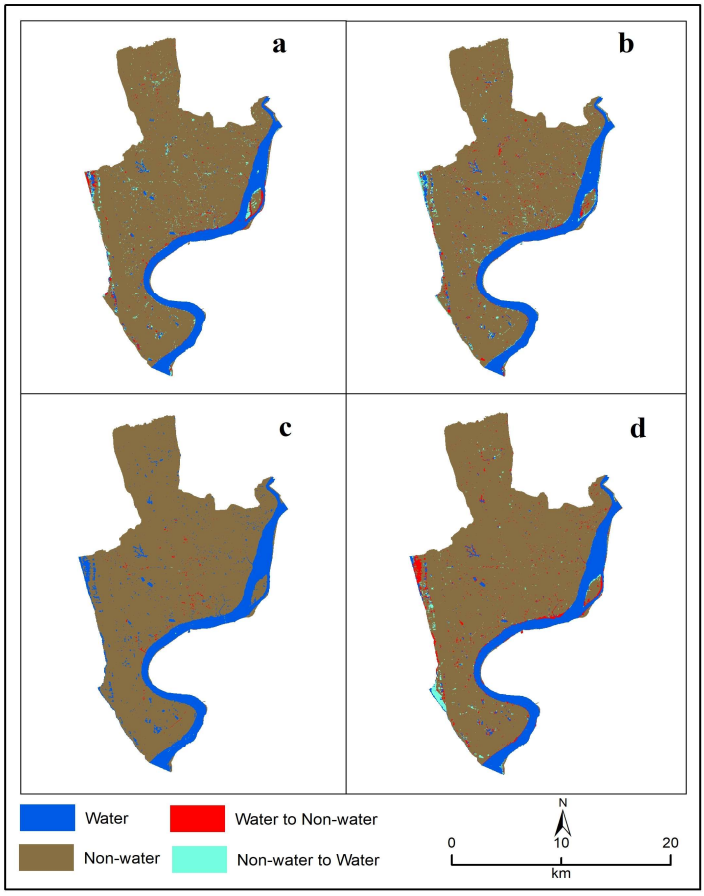

Figure 5.7: Places of water and non-water interaction (2000 to 2020)

Within the last 5 years of change (2015 to 2020) the areas that have been converted from non-water bodies to water bodies was less than that of areas changed from water bodies to non-water bodies.

Within this time, there was no change in 164.792 sq km of non-water bodies, like 24.039 sq km water bodies.

5.4 Water and Non-water Simulation for 2040:

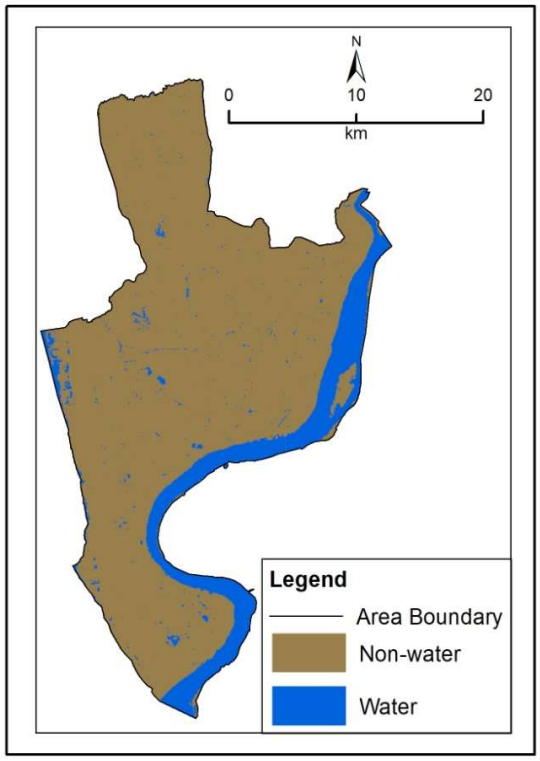

Figure 5.8: Simulated water and non-water bodies for the year 2040

By 2040 water bodies in this city will increase slightly, but the quantity will be very little which will be only one sq km greater than that of 2020. It should be noted that most of the changes will be organized in and around the river and sea. These changes might be resulted from the increment in water level by climate change or the extinction of dunes in the river.

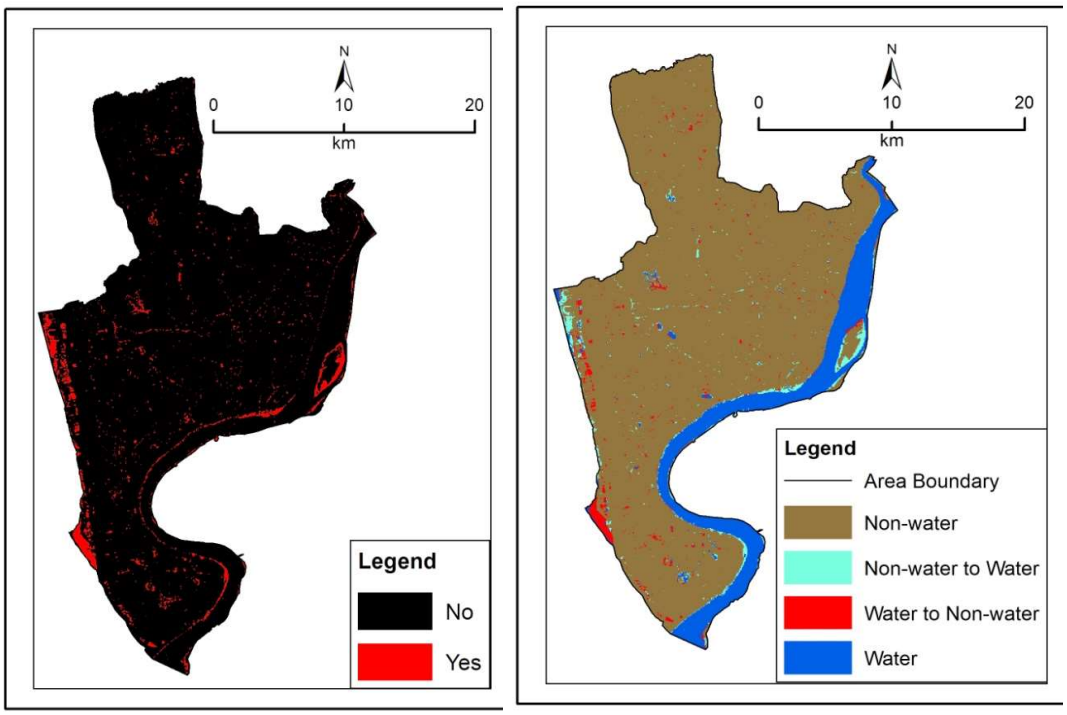

Figure 5.9: Changes in urban water bodies in Chittagong city (2020 - 2040). Boolean map of changes (left), interaction map of water bodies and non- water bodies (right)

Now, if we look at this change from 2020, we can see that about 4.00 sq km of non-water bodies will be changed to water bodies (nearly 2% of the study area). Likewise, 3.022 sq km of the water bodies will be replaced by non-water bodies. Looking at the constant areas, there will be no change in about 165.392 sq km non- water bodies and 23.807 water bodies.

Table 5.4: Interaction between water bodies and non- water (2020 - 2040)

Time	**Area (sq. km)**	**%**
Non-water - Non-water	165.392	84.349
Non-water - Water	3.859	1.968
Water - Non-water	3.022	1.541
Water - Water	23.807	12.141
	196.080	100

CHAPTER SIX
Conclusion and Future Works

6.1 Conclusion

6.2 Future Works

6.1 Conclusion

Water bodies have a much lower conversion tendency in Chittagong than in Dhaka city, although it is the second-largest city and the commercial hub in Bangladesh. There has not been much dramatic change in the entire study period, but as the city's population continues to grow, it will not take long for this to have a Dhaka-like situation. Several studies have proven that the city of Chittagong is suffering from various environmental problems, including water pollution, Which plays a major role in the transformation and disappearance of these urban water bodies. Industrial pollution, in particular, is making urban water bodies unusable. As a result, the number of water bodies is decreasing day by day, and the land-use scenario is changing drastically. In a city, when the construction land expands, the number of heat island also increase. These heat islands ultimately change the climate of the whole city and make the city uninhabitable. So, to secure the existence of the city and its population, it is high time to take the initiative to conserve existing water bodies. This conservation practice requires strict enforcement of existing laws as well as necessary amendments to the law. In addition to the administration, the general public, who are residents of this city should be aware of these issues. To make them aware, this type of scientific study results should be presented to them so that they can see and understand the present situation of these water bodies and what is waiting for the future.

DL is such a powerful tool that can be adopted to observe changes not only in water bodies but also in other natural resources as well. Lastly, it is not right to think that we should always have high-resolution data for environmental resource monitoring. This study has proved that DL is highly capable of extracting information from low-resolution data as well.

6.2 Future Works

The application of deep learning has already been observed in various fields. It is gaining popularity over conventional methods in extracting information from satellite imagery. Applying the deep learning skeleton used in this study, we can explore the environmental problems in more detail. For example, one can take this study a step further by looking at some of the dominant lands uses that are directly and indirectly driving this change. Besides, If a researcher wants, he or she can compare this method with the conventional methods (e.g. indices) to see which one is more effective. The accuracy level of this study is indeed very satisfactory, but its further increment is possible, which will largely depend on the spatial resolution of the data.

Finally, for further utilization, this model can be modified to make a more complex One. For instance, a researcher can build a hybrid model by combining this 2D CNN model with a 3D CNN model, which might help in monitoring the environmental problems in a more precise way.

Bibliography

Ahmed, B., & Dewan, A. (2017). Application of Bivariate and Multivariate Statistical Techniques in Landslide Susceptibility Modeling in Chittagong City Corporation, Bangladesh. Remote Sensing, 9(4), 304. doi:10.3390/rs9040304.

Amidi, A., Amidi, S. Convolutional Neural Networks cheatsheet. Available at: https://stanford.edu/~shervine/teaching/cs-230/cheatsheet-convolutional-neural- networks [Accessed 20 December, 2020].

ArcGIS for Desktop. How Kriging works. Available at : https://desktop.arcgis.com/en/arcmap/10.3/tools/3d-analyst-toolbox/how-kriging-works.htm. [Accessed 12 December, 2020] .

ArcGIS for Desktop. Understanding universal krignig. Available at : https://desktop.arcgis.com/en/arcmap/latest/extensions/geostatistical-analyst/understanding-universal-kriging.htm. [Accessed 12 December, 2020].

BBS. (2011). Population & housing census, national Vol. 3, urban area report, Bangladesh Bureau of Statistics. Ministry of Planning. Government of the People's Republic of Bangladesh, Dhaka, Bangladesh.

BBS. (2013). Economic census, Zila series: Chittagong, Bangladesh Bureau of Statistics. Ministry of Planning. Government of the People's Republic of Bangladesh, Dhaka, Bangladesh.

BMD. (2013). Bangladesh Metrological Department, annual rainfall and temperature analysis. http://www. bmd.gov.bd/. [Accessed 12 December, 2014].

Bogdanets, V., Vlaev, A. (2015). Analysis of land use changes near large water bodies in Ukraine using GIS. Journal of Environmental Biology 36, pp 37-41.

Broadbent, A.M., Coutts, A.M., Tapper, N.J., Demuzere, M., Beringer, J. (2017). The microscale cooling effects of water sensitive urban design and irrigation in a suburban environment. Theor. Appl. Climatol. https://doi.org/10.1007/s00704-017-2241-3.

Brownlee, J. (2017). What is the Difference Between a Parameter and a Hyperparameter?. Available at: https://machinelearningmastery.com/difference-between-a-parameter-and-a-hyperparameter/#:~:text=In%20summary%2C%20model%20parameters%20are,be%20set%20manually%20and%20tuned . [Accessed 22 December, 2020].

Brownlee, J. (2019). A Gentle Introduction to Pooling Layers for Convolutional Neural Networks. Available at: https://machinelearningmastery.com/pooling-layers-for-convolutional-neural-networks/#:~:text=A%20pooling%20layer%20is%20a,Convolutional%20Layer [Accessed 12 December, 2020]

Brownlee, J.(2020). How to Calculate Precision, Recall, and F-Measure for Imbalanced Classification. Available at: https://machinelearningmastery.com/precision-recall-and-f-measure-for-imbalanced-classification/#:~:text=In%20an%20imbalanced%20classification%20problem,true%20positives%20and%20false%20positives.&text=The%20result%20is%20a%20value,for%20full%20or%20perfect%20precision . [Accessed 05 December, 2020].

Cai, Y., Guan, K., Peng, J., Wang, S., Seifert, C., Wardlow, B., & Li, Z. (2018). A high-performance and in-season classification system of field-level crop types using time-series Landsat data and a machine learning approach. Remote Sensing of Environment, 210, 35–47. doi:10.1016/j.rse.2018.02.045

Chen, Y., Lin, Z., Zhao, X., Wang, G., & Gu, Y. (2014). Deep Learning-Based Classification of Hyperspectral Data. IEEE Journal of Selected Topics in Applied Earth Observations and Remote Sensing, 7(6), 2094–2107. doi:10.1109/jstars.2014.2329330

Cireşan, D. C., Meier, U., Gambardella, L. M., & Schmidhuber, J. (2010). Deep, Big, Simple Neural Nets for Handwritten Digit Recognition. Neural Computation, 22(12), 3207–3220. doi:10.1162/neco_a_00052

Denning, J. (1993), Small-government GIS, Civil Engineering. 63(6). pp 52–54.

Di Franco, G., Santurro, M. (2020). Machine learning, artificial neural networks and social research. Quality & Quantity. https://doi.org/10.1007/s11135-020-01037-y

Dive into Deep Learning, n.d. Forward Propagation, Backward Propagation, and Computational Graphs. Available at: https://d2l.ai/chapter_multilayer-perceptrons/backprop.html. [Accessed 22 December, 2020].

Earth Observation System. n.d. LANDSAT 5 (MSS). Available at: https://eos.com/landsat-5-mss/. [Accessed 24 December, 2020].

Earth Observation System. n.d. LANDSAT 5 (TM). Available at: https://eos.com/landsat-5-tm/ . [Accessed 24 December , 2020].

Earth Observation System. n.d. LANDSAT 8. Available at: https://eos.com/landsat-8/ [Accessed 24 December, 2020].

Ganegedara, T. (2018). Intuitive Guide to Convolution Neural Networks. Avaialable at: https://towardsdatascience.com/light-on-math-machine-learning-intuitive-guide-to-convolution-neural-networks-e3f054dd5daa. [Accessed 15 December, 2020].

Geeksforgeeks. (2019). CNN | Introduction to Pooling Layer. Available at: https://www.geeksforgeeks.org/cnn-introduction-to-pooling-layer/. [Accessed 19. December . 2020].

Geng, J., Fan, J., Wang, H., Ma, X., Li, B., & Chen, F. (2015). High-Resolution SAR Image Classification via Deep Convolutional Autoencoders. IEEE Geoscience and Remote Sensing Letters, 12(11), 2351–2355. doi:10.1109/lgrs.2015.2478256

GIS Geography. 2021. Image Classification Techniques In Remote Sensing. Available at: https://gisgeography.com/image-classification-techniques-remote-sensing/#:~:text=1-,Unsupervised%20Classification,is%20the%20most%20basic%20technique. [Accessed 18 January, 2021].

Google Developers n.d. Machine Learning Crash Course. Available at : https://developers.google.com/machine-learning/crash-course/classification/accuracy. [Accesed 15 January, 2021]

Gross, G. (2017). Some effects of water bodies on the environment–numerical experiments. Journal of Heat Island Institute International 12-2.

Hassan, M. M., & Nazem, M. N. I. (2015). Examination of land use/land cover changes, urban growth dynamics, and environmental sustainability in Chittagong city, Bangladesh. Environment, Development and Sustainability, 18(3), 697–716. doi:10.1007/s10668-015-9672-8

Hathway, E. A., and Sharples, S. (2012). The interaction of rivers and urban form in mitigating the Urban Heat Island effect: A UK case study. Building and Environment, 58, 14–22. doi:10.1016/j.buildenv.2012.06.013

Hughes, R. M., Dunham, S., Maas-Hebner, K. G., Yeakley, J. A., Schreck, C., Harte, M., Molina, N., Shock, C, C., Kaczynski, V.W., Schaeffer, J. (2014). A Review of Urban Water Body Challenges and Approaches: (1) Rehabilitation and Remediation. Fisheries, 39(1), 18–29. doi:10.1080/03632415.2013.836500 .

Humboldt State University. (2013). Radiometric Calibration and Corrections. Available at: http://gsp.humboldt.edu/OLM/Courses/GSP_216_Online/lesson4-1/radiometric.html#:~:text=Radiometric%20correction%20is%20done%20to,quality%20of%20remote%20sensed%20data.&text=Therefore%2C%20in%20order%20to%20obtain,errors%20must%20be%20accounted%20for. [Accessed 25 December, 2020].

Hussain, M. R., Paul, A., & Islam, A. (2016). Spatio-Temporal Analysis of Land Use and Land Cover Changes in Chittagong City Corporation, Bangladesh. International Journal of Advancement in Remote Sensing, GIS and Geography. 4(2). 56-72.

Islam, M. S. (2009). Geomorphological control of urban land development and geo-environmental settings in Chittagong city, Bangladesh. Plan Plus, 5, pp 1–11.

Ismail, M. H., Pakhriazad, HZ., & Shahrin, MF. (2009). Evaluating supervised and unsupervised techniques for land cover mapping using remote sensing data. Geografia : Malaysian Journal of Society and Space.

Jet Propulsion Laboratory. n.d. ASTER Global Digital Elevation Map Announcement. Available at: https://asterweb.jpl.nasa.gov/gdem.asp. [Accessed 25 December, 2020]

Jeton, A. E., & Smith, J. L. (1993). DEVELOPMENT OF WATERSIIED MODELS FOR TWO SIERRA NEVADA BASINS USING A GEOGRAPHIC INFORMATION SYSTEM. Journal of the American Water Resources Association, 29(6), 923–932. doi:10.1111/j.1752-1688.1993.tb03253.x

Ji, S., Zhang, C., Xu, A., Shi, Y., & Duan, Y. (2018). 3D Convolutional Neural Networks for Crop Classification with Multi-Temporal Remote Sensing Images. Remote Sensing, 10(2), 75. doi:10.3390/rs10010075

Jordan, M. I., & Mitchell, T. M. (2015). Machine learning: Trends, perspectives, and prospects. Science, 349(6245), 255–260. doi:10.1126/science.aaa8415

LeCun, Y., Bengio, Y., & Hinton, G. (2015). Deep learning. Nature, 521(7553), 436–444. doi:10.1038/nature14539

Macrotrends LLC, n.d. Chittagong, Bangladesh Metro Area Population 1950-2021. Available at: https://www.macrotrends.net/cities/20115/chittagong/population. [Accessed 23 December, 2020].

Malik, N. (2005). National Conference on 'Unearthing Technological Developments & their Transfer for Serving Masses' 17-18 April. GLA ITM, Mathura, India

Manteghi, G., Limit, H. B., & Remaz, D. (2015). Water Bodies an Urban Microclimate: A Review. Modern Applied Science, 9(6). doi:10.5539/mas.v9n6p1

Manteghi, G., Lamit, H., Remaz, D., and Aflaki, A. (2016). ENVI-Met simulation on cooling effect of Melaka River. International Journal of Energy and Environmental Research, 4(2), pp 7–15.

MathWorks . n.d. Batch normalization layer. Available at: https://www.mathworks.com/help/deeplearning/ref/nnet.cnn.layer.batchnormalizationlayer.html. [Accessed 21 December, 2020].

Meszlényi, R. J., Buza, K., & Vidnyánszky, Z. (2017). Resting State fMRI Functional Connectivity-Based Classification Using a Convolutional Neural Network Architecture. Frontiers in Neuroinformatics, 11. doi:10.3389/fninf.2017.00061

Mhatre, M. S., Siddiqui, F., Dongre, M., Paramjit, T. (2015). A Review paper on Artificial Neural Network: A Prediction Technique. International Journal of Scientific & Engineering Research. 6(12).

Milosevic, D., and Winker, M. (2015): The Role of Water for Sustainable Urban Planning. In: Condie, Jenna/Anna Mary Cooper (Ed.): Dialogues of Sustainable Urbanisation. Social Science Research and Transitions to Urban Contexts. Penrith : University of Western Sydney , 248-251

Mnih, V., & Hinton, G. E. (2010). Learning to Detect Roads in High-Resolution Aerial Images. Lecture Notes in Computer Science, 210–223. doi:10.1007/978-3- 642-15567-3_16

Mobahi, H., Collobert, R., & Weston, J. (2009). Deep learning from temporal coherence in video. Proceedings of the 26th Annual International Conference on Machine Learning - ICML '09. doi:10.1145/1553374.1553469

Mostafa, T., and Manteghi. G. (2019). Influential factors of water body to enhance the urban cooling islands (ucis): a review. International Transaction Journal of Engineering, Management, & Applied Sciences & Technologies. 11(2). DOI: 10.14456/ITJEMAST.2020.27

Neelakantan, T. R., & Ramakrishnan, K. (2017). Protection of Urban Water body Infrastructure – Policy Requirements. IOP Conference Series: Earth and Environmental Science, 80, 012068. doi:10.1088/1755-1315/80/1/012068 .

O'Mahony, N., Campbell, S., Carvalho, A., Harapanahalli, S., Hernandez, G. V., Krpalkova, L., Riordan, D., and Walsh, J. (2019). Deep Learning vs. Traditional Computer Vision. Childhood, Science Fiction, and Pedagogy, 128– 144. doi:10.1007/978-3-030-17795-9_10

Peccia, F. (2018). Batch normalization: theory and how to use it with Tensorflow. Available at: https://towardsdatascience.com/batch-normalization-theory-and-how-to-use-it-with-tensorflow-1892ca0173ad#:~:text=Batch%20normalization%20is%20a%20method,variance%20of%20the%20layers%20input. [Accessed 21. December, 2020].

Pokharna, H. (2016). The best explanation of Convolutional Neural Networks on the Internet!. Available at: https://medium.com/technologymadeeasy/the-best-explanation-of-convolutional-neural-networks-on-the-internet-fbb8b1ad5df8. [Accessed 20 December, 2020].

Roy, B., and Saha, P. (2016). Temporal Analysis of Land Use Pattern Changes in Chittagong District of Bangladesh using Google Earth and ArcGIS. Annual Int'l Conference on Chemical Processes, Ecology & Environmental Engineering (ICCPEE'16) April 28-29. Pattaya Thailand.

Schmidt, J., Marques, M. R. G., Botti, S., & Marques, M. A. L. (2019). Recent advances and applications of machine learning in solid-state materials science. Npj Computational Materials, 5(1). doi:10.1038/s41524-019-0221-0

Sharma, P., Gupta, G., Prabhakar, P., Tiwari, S., Kathait, P., Pathak, Y., Mishra, N., & Kumar, S. (2017). LAND USE LAND COVER CHANGE IMPACT ON WATER RESOURCES - A REVIEW. International Journal of Advances in Engineering & Scientific Research .4(2), pp 07- 14. doi.org/10.5281/zenodo.569714 .

Singh, S. P. Fully Connected Layer: The brute force layer of a Machine Learning model. Available at: https://iq.opengenus.org/fully-connected-layer/. [Accessed 19 December, 2020] .

Sun, R., & Chen, L. (2012). How can urban water bodies be designed for climate adaptation? Landscape and Urban Planning, 105(1–2), 27–33. doi: 10.1016/j.landurbplan.2011.11.018

Thompson, M. M., & Mikhail, E. M. (1976). Automation in photogrammetry: Recent developments and applications (1972–1976). Photogrammetria, 32(4), 111–145. doi:10.1016/0031-8663(76)90008-9.

Tsihrintzis, V. A., Hamid, R., & Fuentes, H. R. (1996). Use of Geographic Information Systems (GIS) in water resources: A review. Water Resources Management, 10(4), 251–277. doi:10.1007/bf00508896

Ullah, M. S., and Enan, M, E. (2016). LANDUSE AND LAND COVER CHANGE IN DHAKA METROPOLITAN AREA DURING 1991-2022. Oriental Geographer. 60(1&2). pp 01-18.

USGS. n.d. Landsat 8. Available at: https://www.usgs.gov/core-science-systems/nli/landsat/landsat-8?qt-science_support_page_related_con=0#qt-science_support_page_related_con. [Accessed 24 December, 2020].

Udapa A., Thukaram, D., and Parthasarathy, K. (1997) "An ANN Based Approach for Voltage Stability Assessment", International Conference on Computer Applications in Electrical Engineering, September. 8. pp. 666–670.

Udofia, U. (2018). Basic Overview Of Convolutional Neural Network (CNN). Available at: <https://medium.com/dataseries/basic-overview-of-convolutional- neural-network-cnn-4fcc7dbb4f17#:~:text=The%20activation%20function%20is%20a,of%20neurons%20as%20input.%E2%80%9D%20%E2%80%94> [Accessed 02 January, 2021].

USGS, n.d. Landsat 5. Available at: https://www.usgs.gov/core-science-systems/nli/landsat/landsat-5?qt-science_support_page_related_con=0#qt-science_support_page_related_con. [Accessed 24 December, 2020)

Verma, S. (2019). Understanding different Loss Functions for Neural Networks. Available at: https://towardsdatascience.com/understanding-different-loss-functions-for-neural-networks-dd1ed0274718 . [Accessed 22 December, 2020]

Weng, Q., & Yang, S. (2004). Managing the adverse thermal effects of urban development in a densely populated Chinese city. Journal of Environmental Management, 70(2), 145–156. doi:10.1016/j.jenvman.2003.11.006

Xu, H. (2006). Modification of normalised difference water index (NDWI) to enhance open water features in remotely sensed imagery. International Journal of Remote Sensing, 27(14), 3025–3033. doi:10.1080/01431160600589179

Yang, B., Meng, F., Ke, X., & Ma, C. (2015). The Impact Analysis of Water Body Landscape Pattern on Urban Heat Island: A Case Study of Wuhan City. Advances in Meteorology, 2015, 1–7. doi:10.1155/2015/416728

Zhang, F., Du, B., & Zhang, L. (2015). Saliency-Guided Unsupervised Feature Learning for Scene Classification. IEEE Transactions on Geoscience and Remote Sensing, 53(4), 2175–2184. doi:10.1109/tgrs.2014.2357078

Zhang, F., Du, B., & Zhang, L. (2016). Scene Classification via a Gradient Boosting Random Convolutional Network Framework. IEEE Transactions on Geoscience and Remote Sensing, 54(3), 1793–1802. doi:10.1109/tgrs.2015.2488681

Zhang, M., Lin, H., Wang, G., Sun, H., & Fu, J. (2018). Mapping Paddy Rice Using a Convolutional Neural Network (CNN) with Landsat 8 Datasets in the Dongting Lake Area, China. Remote Sensing, 10(11), 1840. doi:10.3390/rs10111840

50 North | GIS blog from Ukraine. 2017. How To Pick The Best Supervised Classification Method?. Available at: http://www.50northspatial.org/pick-best-supervised-classification-method/. [Accessed 18 January, 2021].

Masters Program in **Geospatial Technologies**

Supported by:
Education and Culture
ERASMUS MUNDUS